JOURNAL
OF
GEOMAGNETISM
AND
GEOELECTRICITY

VOL. VI NO. 3

SOCIETY
OF
TERRESTRIAL MAGNETISM AND ELECTRICITY
OF
JAPAN

SEPTEMBER 1954
KYOTO

JOURNAL OF GEOMAGNETISM AND GEOELECTRICITY

EDITORIAL OFFICE: Society of Terrestrial Magnetism and Electricity of Japan, Geophysical Institute, Kyoto University, Kyoto, Japan

The fields of interest of this quarterly Journal are as follows:

Terrestrial Magnetism	Aurora and Night Airglow
Atmospheric Electricity	The Ozone Layer
The Ionosphere	Physical States of the Upper Atmosphere
Radio Wave Propagation	Solar Phenomena relating to the above Subjects
Cosmic Rays	Electricity within the Earth

The text should be written in English, German or French. The price is set as 1 dollar per number. We hope to exchange this Journal with periodical publications of any kind in the field of natural science.

The Editors

On Anomalous Variations of Maximum Electron Density and its Height in the $F2$ Region of the Ionosphere

By Teruo SATO

Geophysical Institute, Kyoto University, Kyoto

Abstract

An explanation of anomalous variations of the maximum electron density (proportinal to $(f_0F2)^2$) and its height (h_pF2) of the $F2$ region is attempted. For this purpose, the reexamination of the behaviours of f_0F2, h_pF2 and $h'F2$ in three seasons during sunspot maximum and minimum, is made and some interesting results are obtained. They are the followings. (i) The geomagnetic control of f_0F2 is conspicuous in low and middle latitudes in there seasons. But above middle latitudes the geographic control is remarkable. This is applied above 30° in winter (greatest $\sec\chi$) and equinox. (ii) f_0F2 above 20° in December distributes approximately in such a way as $f_0F2 \propto \cos^{\frac{1}{2}}\chi$ during sunspot minimum, but its distribution during sunspot maximum deviates from this line. (iii) The greater the zenith angle, the greater the increase of electron density from s.s. min. to s.s. max., and thus the magnitude of the seasonal anomaly of f_0F2 is amplified far more during sunspot maximum than the minimum (iv) The value of h_pF2 is greatest at geomagnetic equator throughout the year. (v) h_pF2 becomes larger during sunspot maximum than the minimum. (vi) h_pF2 in December does not increase at higher latitudes and rather decreases.

From these facts it seems that the variations of f_0F2 and h_pF2 are controlled not only by the geomagnetic cause, but also by the cause which relates to the geographic latitude or solar activity. We investingate the geomagnetic distortion of daily variation of electron density due to the vertical electron drift, taking the diurnal and semi-durnal components into consideration, and show that the trough in geomagnetic equator can be explained by this drift. The velocities of two kinds of drift are deduced directly from the data. A reason for geographic control is described. It is shown that the seasonal anomaly of f_0F2 cannot be accounted for only by the vertical drift. Therefore in order to explain the seasonal anomaly of f_0F2 and other phenomena, (iii)–(iv), mentioned

above, we suggest that there is at least the seasonal variation of the height distribution of the particle responsible for the $F2$ region.

1. Introduction

It has been well known that the seasonal and daily variations of f_0F2 (critical frequency of the $F2$ region) and h_pF2 (height of the maximum electron density) of the $F2$ region) deviate remarkably from the law suggested by Chapmam [1]. One way to explain these anomalies is the thermal expantion of the region ([2], [3], [4]). However, the variation of the temperature to explain these anomalies is very great, therefore is not acceptable physically [5]. The variation due to the diffusion of an electron was considered by Ferraro [6]. According to his calculation the variation of the electron density due to this effect is very small even in the $F2$ region. The number density of particle taken by him is of two kinds. For smaller number density of particle the variation will become greater than that of his computation. But there still remains a doubt as to the behaviour of h_pF2.

Another excellent theory is the vertical electron drift by the electro-dynamic force firstly suggested and calculated by Martyn [7] and followed by Weiss [8] and Maeda [9]. This theory is qualitatively correct. It appears, however, that no satisfactory results have been found.

Our recent study of the latitudinal distribution of f_0F2 and h_pF2 shows, besides the geomagnetic control of f_0F2 which supported the drift theory, there is a geographic control in middle and higher latitudes, and the anomalies have a relation with the solar activity. Therefore we consider that the various kinds of anomalous variations are ascribed to the sum of the geomagnetic and the geographic causes. It seems that at certain place and time the former is predominant; and at another, the latter. In this paper, therefore, we first investigate whether or not the anomalies under the geomagnetic control can be accounted for by the vertical electron drift, and next in order to explain the anomalies which can not be explained by the electron drift, a suggestion is made.

2. Statistical Results of Distributions of f_0F2, $h'F2$ and h_pF2

For the purpose of well understanding and of later discussions we show in Fig. 1 (a)–(f) the latitudinal distribution of the value of f_0F2, h_pF2 and $h'F2$ (the minimum virtual height of the $F2$ region) at noon during the sunsopt maximum (s.s. max.) and minimum (s.s. min.). The upper two part in each fignre are respectively the distribution of f_0F2 in geomagnetic and geographic latitudes, while the lower distributions are respectively the distribution of $h'F2$ (cross) and h_pF2, (square) which are derived by Shimazaki's [10] method, using the value of M(3000)$F2$. in geomagnetic latitude. The data subjected to statistics are the hourly median values in Sep., Dec., 1947, Jun. 1948 and Jun., Sep., Dec. 1953. Jun., Sep., Dec. are the representatives of three seasons, the summer (May., Jun., Jul., Aug.), the equinox (Mar., Apr., Sep., Oct.) and the winter (Jan., Feb., Nov., Dec.).

It has been known that the value of f_0F2 shows less scatter when plotted in the geomagnetic latitude than in geographic ([11], [12], [13], [14],). But our

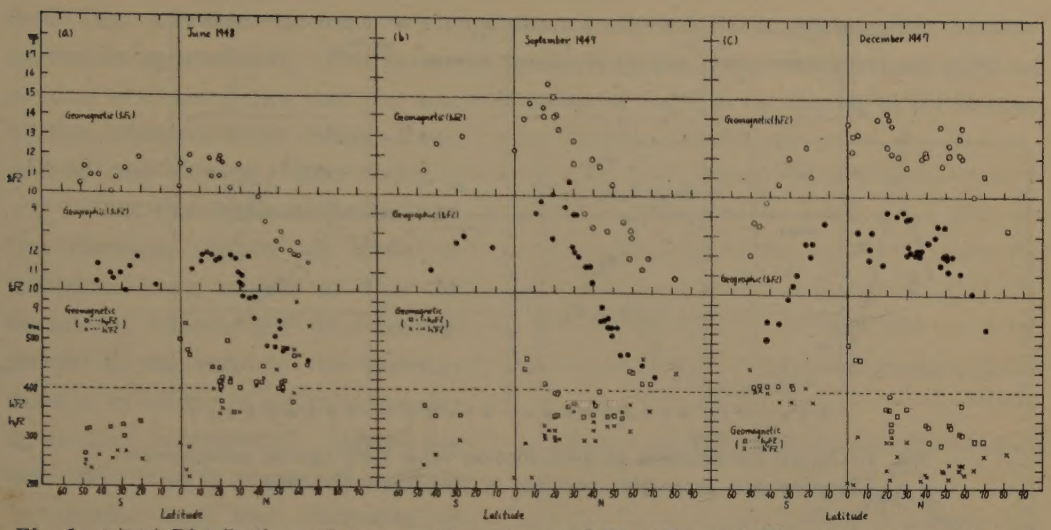

Fig. 1 (a)-(c) Distributions of noon median values of f_0F2, $h'F2$ and h_pF2 against geomagnetic and geographic (only f_0F2) latitndes. Period corresponds to sunspot maximum.

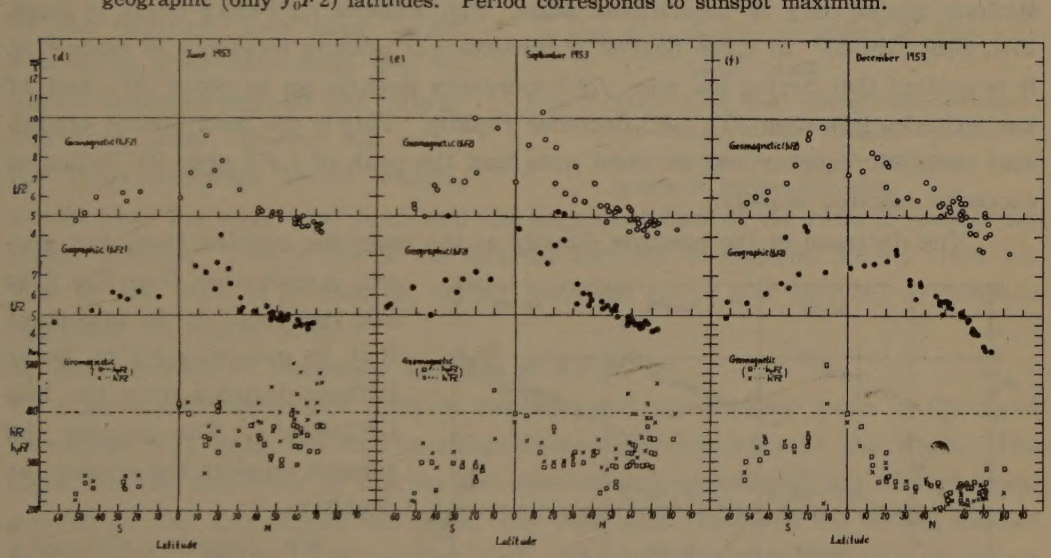

Fig. 1 (d)-(f) Distributions of noon median values of f_0F2, $h'F2$, and h_pF2 against geomagnetic and geographic (only f_0F2) latitudes. Period corresponds to sunspot minimum.

detailed statistics show that though the above is consistent with our distribtion of f_0F2 in low and middle latitudes in geographic, the value of f_0F2 above middle latitudes show better distributions in geographic than in geomagnetic. Especially, this is clearly seen in Dec. 1953 in northern hemisphere. The data in Dec. and Sep. 1952 and 1951 show the same result (Fig. 1 (A), (B), only for Dec.) There is a tendency that the smaller the average zenith angle at noon, of the month the better the geographic distribution.

We have a reason to believe, as shown below, that in winter (greatest zenith angle) the value of f_0F2 is well distributed in geographic latitude, even if the electron drift is present. Hence we plotted the value of f_0F2 at noon at various

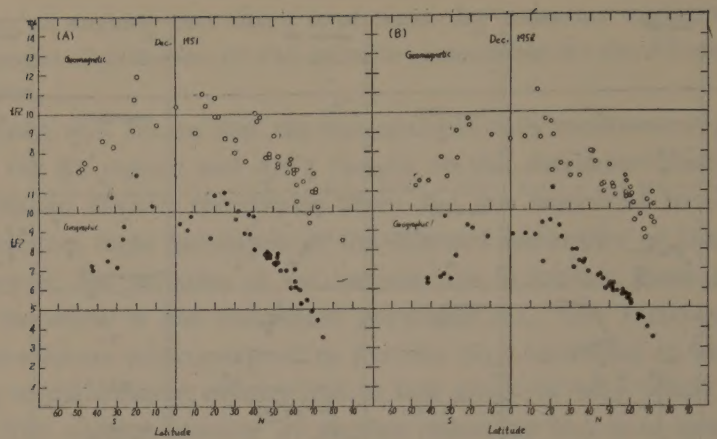

Fig. 1 (A) (B) Distributions of noon median value f_0F2 against geomagnetic (uppes) and geographic latitudes in Decs. 1951 and 1952.

stations agaist $\cos\chi$ in logarithmic scale. Fig. 2 shows f_0F2-$\cos\chi$ curve in Decs. 1947, 1949, 1951–53. In these figures, a correction of grazing incidence is made [15]. It is evident that during s.s. mim. f_0F2 increases linearly up to about 20°, and at low latitudes less than 20°, f_0F2 decrease rapidly. This is the well known trough near magnetic equator and we must note that the peak of f_0F2 near 20° indicates excessive electron density.

The decrease of the electron density at the magnetic equator from the normal is estimated, from Fig. 2, as fifty percent. It is important that in general f_0F2 in lower latitude deviates from the line $f_0F2 \propto \cos^{\frac{1}{2}}\chi$. The greater the sunspot number, the greater the deviation.

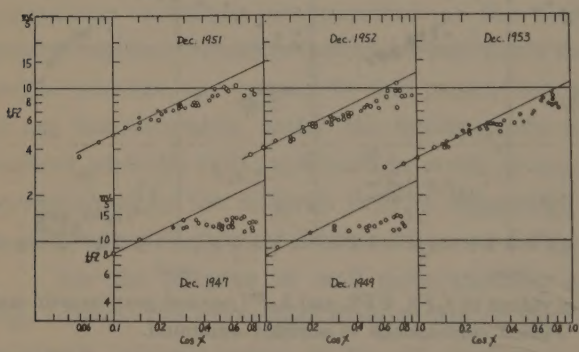

Fig. 2 Distribution of noon median value of f_0F2 in various latitudes (northern hemisphere) against $\cos\chi$. Full line represents $f_0F2 \propto \cos^{\frac{1}{2}}\chi$.

We regard $f_0F2 \propto \cos^{\frac{1}{2}}\chi$ as usual relation, based on later discussion. It is considered that if the $F2$ region is formed by a different radiation from that of the $F1$ region and decay of the electron is of an attachment type, above relation is possible, but if the $F2$ region is formed in such a way as Bradbury's [16] hypothesis, the above relation does not hold. This is because the production of the electron near the maximum of the $F2$ region in various latitudes is not so much different one another for the latter theory. However, above inferences are, needless to say, not decisive.

There are also such notable characteristics as h_pF2 being greatest at geomagnetic (or magnetic equator), and in general h_pF2 increases far more during s.s.

max. than s.s. min. through two hemispheres, while $h'F2$ in geomagnetic equator decreases appreciablly. The harmonic analysis of the daily variation of h_pF2 at several stations shows that the augumentation of h_pF2 is attributed to an incease of the constant trem (mean level) and not the sineand cosine terms.

Next Fig. 3 shows the ratio of the electron density at noon of minimum $\cos\chi$ month to that of maximum. Above 23.5° this corresponds to the ratio of the electron density in winter to summr (opposite in souther hemisphere). During s.s. min. this ratio is greater than untiy in middle and high latitudes in northern hemisphere and at the rest of the stations less than unity. Especially, it is interesting that in higher latitudes than 60 this ratio is less than unity. During s.s. max., the ratio increases world widely, except near the equatorial zone, and the augumentation of the ratio is greater for higher latitdes. This is due to the fact the increase of electron density from s.s. min. to s.s. max. is greatest in winter (smallest $\cos\chi$) and smallest in summer (including equatorial zone)

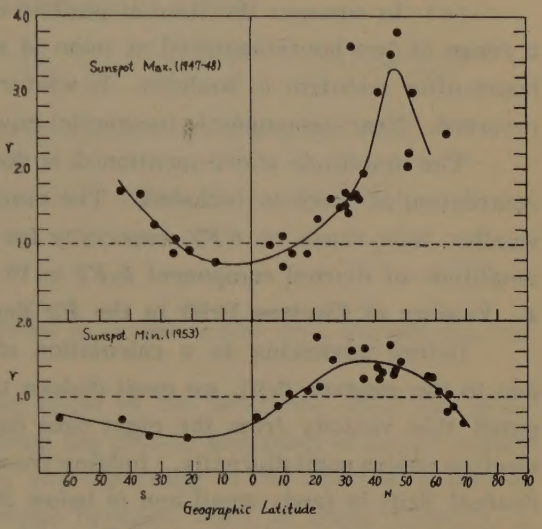

Fig. 3 Ratio (r) of noon median value of electron density of the $F2$ region in minimum $\cos\chi$ month to that in maximum $\cos\chi$ month in various latitudes.

3. Some Results of Harmonic Analysis of $h'F2$

Harmonic analysis of $h'F2$ in summer and winter was made by Sato and Namikawa [17], using the data in about thirty observatories over the world. The phase and the amplitude of diurnal and semi-diurnal components are plotted agaist geographic and geomagetic latitudes. The data used there are the hourly median values of $h'F2$ in Jun., 1946 and Dec. 1945. The daily variation of $h'F2$ is analogous to that of h_pF2, so that we can utilize these results. The results of analysis are summarized in the following.

(i) In summer the amplitude of the diurnal component is greater in northern hemisphere than in southern and *vice versa* in winter.

(ii) The amplitude of semi-diurnal component has an anologous distribution through two hemispheres as that in (i). But the difference of amplitude between two hemispheres at any solstice is smaller than that in the diurnal.

(iii) The amplitude of diurnal component is greater than that of semi-diurnal in summer (winter) and is comparable with or slightly greater than that in winter (summer) in northern (southern) hemisphere. The magnitude of two components are respectively 50–70km and 30–40km in summer and 20–30km and 10–20km in winter.

(iv) The time of positive maximum of semi-diurnal component is within a range of one or two hours centered and at noon at midnight two hemispheres in two solstices.

(v) In summer the time of positive maximum of diurnal component is within a range of two hours centered at noon in northern hemisphere and is within two hours after midnight in souhern. In winter these circumstances are approximately reversed. Near geomagnetic (magnetic) equator, the phase differs by 4–5 hours.

The amplitude above mentioned is doubt, because the influence such as the retardation of wave is included. The amplitudes of two components of h_pF2 are smaller than those of $h'F2$, especially for high latitude. Near magnetic pole the amplitude of diurnal component h_pF2 is 10–20km.

4. Velocity of Electron Drift in the $F2$ Region

Before advancing to a calculation of the variation of the electron densitiy due to the electron drift, we must deduce the velocity itself. Mitra [18] has computed this velocity from the night time data of the $F2$ region, assuming that the electron moves semi-diurnally. Judging from their results the velocity of the semi-drurnal drift is fairly small and is below 20km/hr. In this section we will obtain the velocity of not only the semi-diurnal but also the diurnal, by a method which is different from that of him.

It we use the attachment law for the electron decay, the variaton of the electron density is given by

$$\frac{\partial N}{\partial t}=q-\beta N-v\frac{\partial N}{\partial z}, \tag{1}$$

where q is the electron production per c.c. per sec., v, the drift velocity of the electron which is independent of height, z, the coordinate of the height in unit of scale height. β, strictly speaking, is not the attachment coefficient, but hereafter we call this as the attachment coefficient for the sake of convenience. We assume that the velocity of the electron is given by

$$v=v_1\sin(\omega t+\lambda_1)+v_2\sin(2\omega t+\lambda_2), \qquad \omega=15^\circ/\text{hr}. \tag{2}$$

where v_1 and v_2 represent respectively the constant amplitude of two kinds of velocity and λ_1, λ_2 are phase lags. Substituting (2) into (1) and integrating the two sides of the equation from t_1 to t_2 and from t_2 to t_3, we obtain two expressions. If the latter expression is subtracted from the former, the term concerning the electron production is eliminated when $|t_1-t_2|=|t_2-t_3|$ and we take t_2 as noon. Then we obtain the following expresson.

$$\int_{t_1}^{t_2}\frac{\partial N}{\partial t}dt-\int_{t_2}^{t_3}\frac{\partial N}{\partial t}dt=-\beta\left[\int_{t_1}^{t_2}Ndt-\int_{t_2}^{t_3}Ndt\right]-\left[\int_{t_1}^{t_2}v\frac{\partial N}{\partial z}dt-\int_{t_2}^{t_3}v\frac{\partial N}{\partial z}dt\right]. \tag{3}$$

where β is regarded independent of the height. Now we assume that the distribution of the electron density during the integration is Chapman's form, i.e.,

$$N=N_0e^{\frac{1}{2}(1-z-e^{-z})}, \tag{4}$$

then

$$\frac{\partial N}{\partial z} = N_0 e^{\frac{1}{2}(1-z-e^{-z})} \cdot \frac{1}{2}(-1+e^{-z}). \tag{5}$$

Thus the expression (3) is writtien approximately as follows;

$$N|_{t_1}^{t_2} - N|_{t_2}^{t_3} = -\beta\left[\frac{N_{t_1}+N_{t_2}}{2} - \frac{N_{t_2}+N_{t_3}}{2}\right](t_2-t_1) + \frac{1}{\omega}\left[\frac{N_{t_1}+N_{t_2}}{2} \cdot \frac{1}{2}(1-e^{-z})_{t_{1,2}}\right.$$
$$\times \left\{v_1\cos(\omega t_1+\lambda_1) + \frac{1}{2}v_2\cos(2\omega t_1+\lambda_2) - v_1\cos(\omega t_2+\lambda_1) - \frac{1}{2}\cos(2\omega t_2+\lambda_2)\right\}$$
$$- \frac{N_{t_2}+N_{t_3}}{2} \cdot \frac{1}{2}(1-e^{-z})_{t_{2,3}}\left\{v_1\cos(\omega t_2+\lambda_1) + \frac{1}{2}v_2(2\omega t_2+\lambda_2) - v_1\cos(\omega t_3+\lambda_1)\right.$$
$$\left.\left. - \frac{1}{2}v_2\cos(2\omega t_3+\lambda_2)\right\}\right]. \tag{6}$$

where the value at $t_{1,2}$ is the mean of those at t_1 and t_2 and N_{t_1}, N_{t_2} and N_{t_3} are considered approximately equal.

In oreder to deduce the velocity we adopt as the reference level the minimum virtual height of the $F2$ region. Since the critical frequency of the $F1$ region (f_0F1) is about equal to the frequency corresponding to the electron density at that height of the $F2$ region (the difference between them is about 0.5mc/s), it appeears that the electron densitiy at $h'F2$ is equal to that corresponding to the frequency ($f_0F1+0.5$)mc/s. At night the electron production is zero. Hence it is only sufficient to integrate the equation (1) from t_1 to t_2 of any time. In that case the electron density at $h'F2$ is that corresponding to the frequency $f_{min}F$ (minimum frequency reflected from the F region).

It is noted that in progress of the calculation the electron density converted to a certain height should be used throughout the time of integration. The phase lags λ_1 and λ_2 are obtained directly from the analysis of the same data from which the velocities v_1 and v_2 are calculated.

The velocities of the diurnal and semi-diurnal drift at Kokubunji, Washington and Watheroo are shown in Table 1. At Kokubunji, two velocities are deduced from day and night time data. The data used here are the average of hourly median values of each month from Jan. 1950 to Dec. 1952. From the results in Table 1, it is found that v_2 is about 4–6m/s which almost equals to the value

Table 1

	Kokubunji				Washington		Watheroo	
	day		night		day		day	
	v_1	v_2	v_1	v_2	v_1	v_2	v_1	v_2
	m/s	m/s	m/s	m/s	m/s	m/s	m/s	m/s
Summer Sol. (May-Aug.)	3.0	4.6	3.2	6.0	6.5	4.3	1.6	3.3
Equinox (Mar. Apr., Sep., Oct.)	1.4	5.2	1.3	5.4	1.8	4.2	1.7	3.2
Winter. Sol. (Jan., Feb., Nov., Dec.)	2.3	4.6	2.5	5.0	2.3	4.5	4.0	4.2

obtained by Mitra. In general v_1 is about half of v_2 in winter and equinox at middle latitudes, while in summer v_1 is comparable with or greater than above and reaches to 6m/s. This fact shows that in summer the diurnal drift mainly contributes to the removal of the electron in middle and high latitudes. This state is consistent with the results obtained by harmonic analysis of $h'F2$. Near the geomagnetic equator, the behaviour of $h'F2$ is slightly different from that of h_pF2. Hence above method cannot be applied. But judging from the variation of h_pF2, the diurnal velocity is probably greater than that in middle latitude and is 5–8m/s.

5. Distortion of Maximum Electron Density Caused by Electron Drift

In the previous section it was found that the diurnal drift is predominant over the semi-diurnal in summer (winter) in northern (southern) hemisphere. The distortion of the electron density so far investigated was for the semi-diurnal drift. In the present section we cmpute effect of two kinds of drift. The equation of the variation of the electron density is

$$\frac{\partial N}{\partial t} = q - \beta N - v\frac{\partial N}{\partial z} \tag{1}$$

The electron production q is the function of the time and the height, and it is difficult to separate the two terms. For the convenience of the calculation we assume that

$$q = q_0 \cos\chi\, e^{(1-z-e^{-z})} = q_0(a + b\sin\omega t)\, e^{(1-z-e^{-z})} \tag{7}$$

where q_0 is the electron production at $z=0$ and $\chi=0$. a and b are constants which depend on the latitude. The assumption (7) implies that the production of the electron varies with $\cos\chi$ while the level of the maxmum production does not vary during the daytime. This invariance of the production level does not agree with the actual state which is usually repersented by Chapman's law. According to the result of calculation in the case of no drift, variation of the electron density in the presence of drift under the condition of (7) appears to behave approximately as in the case of such a production as denoted by Chapman's law. But the height variation at sunrise and sunset may differ from those in Chapman's productions, especially for the electron drift which begins at the same time as the electron production takes place, though such a difference is not much an important problem here. Hence our calculations show a satisfactory result.

We must also know the magnitude of β at any height. It is considered that β can be obtained using the expression (6) by the method of least square. But the magnitude of β thus obtained is very small and sometimes has the minus sign. So that the value is not reliable. Therefore we computed this value from the expression $\beta = -\dfrac{\partial N/\partial t}{N}$, which is applied to the night time ionospheric data. N is the maximum electron density when the height of the maximum does not much vary. The value of β thus obtained is 1.5×10^{-5}/s at Kokubunji; 2.2×10^{-5}/s, at Washington; and 1.7×10^{-5}/s, at Watheroo at the level of 300km.

Now since the velocity of the drift and the value of β are known, we advance

to compute the distortion of the electron density for the following two cases.

$$\begin{array}{lll} (1) & z\geqslant 0 & \beta=1\times10^{-5} \\ & z<0 & \beta=1\times10^{-5}e^{-z} \\ (2) & z\geqslant 0 & \beta=2.72\times10^{-5} \\ & z<0 & \beta=2.72\times10^{-5}e^{-z} \end{array} \qquad (8)$$

(i) Semi-Diurnal Drift

The velocity of the drift is given by

$$v=v_0\sin(2\omega t+\lambda), \qquad (9)$$

where λ is the phase lag and v_0 is constant. We divide the region into thin layer with constant density. Under such a condition the solution of (1) is given by

$$N=q(z)\left(\frac{a}{\beta(z)}+\frac{b(\beta(z)\sin\omega t-\omega\cos\omega t)}{(\beta(z))^2+(\omega)^2}\right)+\left[q(p)\left(\frac{-a}{\beta(p)}+\frac{\omega}{(\omega)^2+(\beta(p))^2}+Q(p)\right]e^{-\beta(z)t}, \qquad (10)$$

where $$p=z-\frac{v_0}{2\omega}[1-\cos(2\omega t+\lambda)], \qquad q(z)=q_0e^{(1-z-e^{-z})}, \qquad (11)$$

and Q is the distributon of the electron density at $t=0$ ($06^h\,00^m$). $\beta(z)$, $q(z)$, $Q(z)$ implies that they are the function of z, and $\beta(p)$, $q(p)$, $Q(p)$ show that z is replaced by p. The daily variation of the electron density for two distributions of β and for $a=0$,

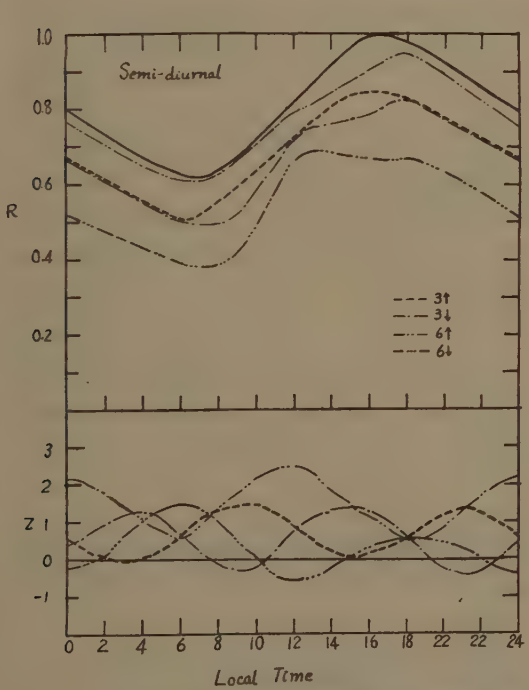

Fig. 4 Daily variations of electron density and height of the moving region with uniform velocity. Full line represents the variation of the static region (no drift) and R represents ratio of electron density at any time to the maxiumum of the static region. $\beta=1\times10^{-5}$/s for $z\geqslant0$, $\beta=1\times10^{-5}e^{-z}$/s for $z<0$.

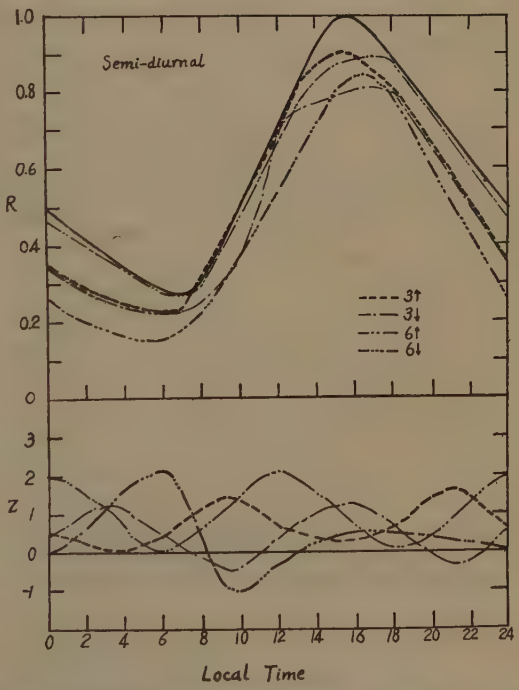

Fig. 5 Daily variations of electron density and height of the moving region with uniform velocity. Full line represents the variation of the static region (no drift) and R represents ratio of electron density at any time to the maxmum of the static region. $\beta=2.72\times10^{-5}$/s for $z\geqslant0$; $\beta=2.72\times10^{-5}e^{-z}$/s for $z<0$.

$b=1$ are shown in Figs. 4 and 5, in which the figures attached to the curves represent the time when the electron begins to move upwards or downwards. For example 0↑ represents the electron drift which begins to move upwards at $00^h\,00^m$. The drift velocity used here is $\frac{v_0}{\omega}=4$ which corresponds to 7.2m/s for H (scale height) $=50$km. The full line represents the variation in the case of no drift, which is called the static region. R is the ratio of electron density at any time to the maximum density of the day of the static region.

It is clear from these figures that the smaller β, the greater the effect. It appears that the variation of height of maximum density obeys well to the movement of the electron. If we adopt far greater value of β than that used here, for example $\beta=1\times10^{-4}$/s, the effect of the drift is remarkably decreased and both the electron density and the height become closely similar to those of the static region.

It is natural but important that the ratio of electron density at sunrise to the maximum of the day becomes greater for greater value of β and that the maximum density itself smaller. In the present, the maximum density in the static

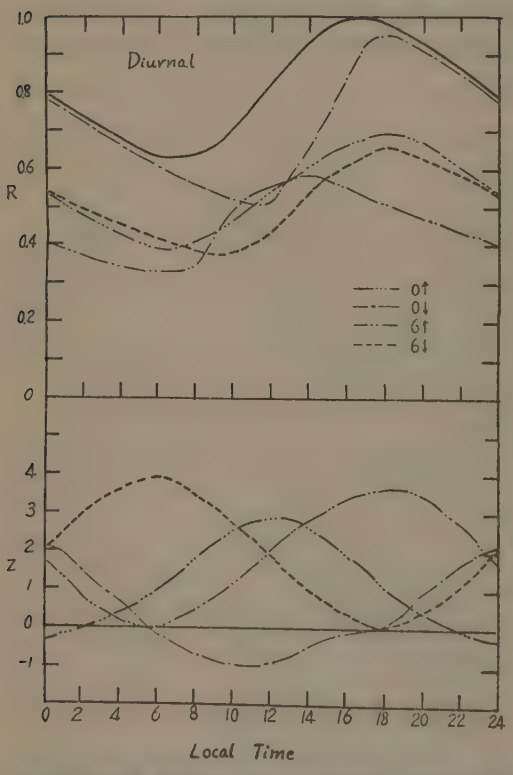

Fig. 6 Daily variation of electron density and height of the moving region with uniform velocity. Full line represents the variation of the sttaic region (no drift) and R represents ratio of electron density at any time to the maximum of static region. $\beta=1\times10^{-5}$/s for $z\geqq0$; $\beta=1\times10^{-5}e^{-z}$/s for $z<0$.

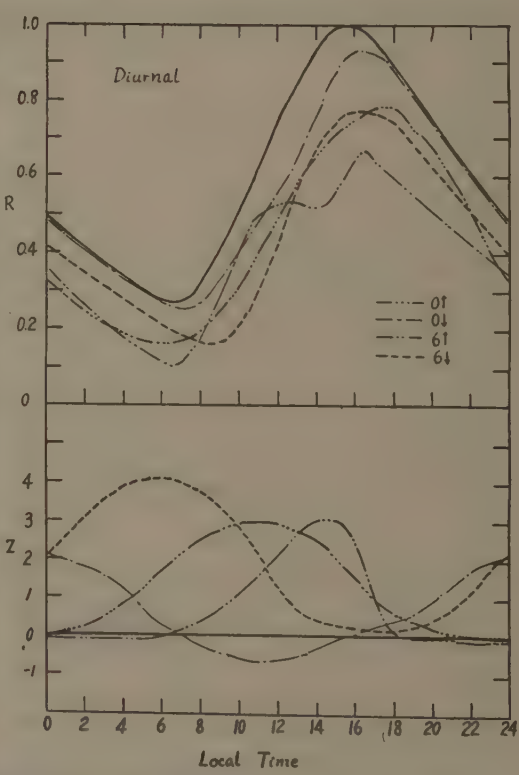

Fig. 7 Daily variation of electron density and height of the moving region with uniform velocity. Full line represents the variation of the static region (no drift) and R represents ratio of electron density at any time to the maximum of static region. $\beta=2.72\times10^{-5}$/s for $z\geqq0$; $\beta=2.72\times10^{-5}e^{-z}$/s for $z<0$.

region is respectively $3.8\times10^4 q_0$ and $1.93\times10^4 q_0$ for cases (1) and (2). If the maximum density of the $F2$ region is 1.5×10^6/c.c. then $q=37\,\mathrm{cm^3/s}$ and $75\,\mathrm{cm^3/s}$. The latter is approximatly equal to the electron production of the $F2$ region generally accepted (for example, Bates [19]).

(ii) Diurnal Drift

The velocity of the drift is given by $v=v_0\sin(\omega t+\lambda)$. Then the variation of the electron density is represented by the same expression as (10). The distribution of β is taken as same as (8). The results are shown in Figs. 6 and 7. It is evident drift gives far more influence than the semi-diurnal, and the electron drift of 6↑ is most effective. The reduction of the electron density relative to the static region reaches about fifty percent.

According to the results mentioned in § 3, the diurnal compnent in summer and winter appears to correspond with the diurnal drift which begins respectvely to move up and down at midnight in northern himisphere. The variations of the height for 0↑ and 0↓ shown in Figs. 6 and 7 agree well with the diurnal components of $h'F2$. Therefore the electron may begin to move up and down at midnight in actual state. It may be considered, however, that as the radiation from the sun produces electron at high level at sunrise, the height for 6↑ rises more rapidly after the sunrise than that shown in Fig 7. In such a circumstance, the diurnal component of the daily variation of $h'F2$ may show also an apparent rise at midnight.

6. Election Drift in Atmosphere of Non-Uniform Temperature

It is intereting to investigate an effect of the temperature with height gradient on the electron density when drift is occuring. Let the temperature increases linearly with height gradient γ.

Then
$$T=T_0+\gamma(h-h_0) \tag{12}$$

where T_0 is the temperature at the reference height h_0. The variation of the electron density is given by

$$\frac{\partial N}{\partial t}=q-\beta N-v\frac{\partial N}{\partial z}-v\frac{N}{T}\frac{\partial T}{\partial z} \tag{13}$$

We use the similar approximate method as in § 5. For the diurnal drift, to which the velocity is given by $v=v_0\sin(\omega t+\lambda)$, the solution of (13) is obtained as follows:

$$N=\left\{-\frac{q(z)}{\omega}\left[\left(\frac{\pi\beta(z)}{2\omega}+1\right)\cos\omega t-\frac{1}{2}\cos^2\omega t\left(\frac{1.5\beta(z)}{\omega}+\frac{\gamma v_0}{\omega T(z)}\right)\right]+Q(p)e^{-\frac{\gamma v_0}{\omega}T(p)}\right.$$
$$\left.+\frac{q(p)}{\omega}\left[\left(\frac{\pi\beta(p)}{2\omega}+1\right)-\frac{1}{2}\left(\frac{1.5\beta(p)}{\omega}+\frac{\gamma v_0}{\omega T(p)}\right)\right]\right\}e^{-\beta(z)t+\frac{\gamma v_0}{\omega}T(z)\cos\omega t},\ \text{for } \lambda=0, \tag{14}$$

where
$$p=z-\frac{v_0}{\omega}(1-\cos\omega t),$$

and

$$N=-\frac{q(z)}{\omega}\cos\omega t-\left\{\frac{\beta(z)}{\omega}\left[\sin\omega t\left(\frac{\beta(z)\pi}{\omega}+1\right)-\frac{1}{2}\sin^2\omega t\left(\frac{1.5\beta(z)}{\omega}-\frac{\gamma v_0}{\omega T(z)}\right)\right]\right.$$
$$-\frac{\gamma v_0}{\omega T(z)}\left[\left(\sin\omega t-\frac{1}{5}\sin^5\omega t\right)\left(\frac{\beta(z)\pi}{\omega}+1\right)-\left(\frac{1}{2}\sin^2\omega t-\frac{1}{6}\sin^6\omega t\right)\right.$$
$$\left.\left.\times\left(\frac{1.5\beta(z)}{\omega}+\frac{\gamma v_0}{\omega T(z)}\right)\right]\right\}e^{-\beta t-\frac{\gamma v_0}{\omega T(z)}\sin\omega t}+\left(Q(p)+\frac{q(p)}{\omega}\right)e^{-\beta(z)t-\frac{\gamma v_0}{\omega T(z)}\sin\omega t},$$

$$\text{for}\quad \lambda=+\frac{\pi}{2}, \tag{15}$$

where $$p=z-\frac{v_0}{\omega}\sin\omega t.$$

When $\lambda=\pi$ and $\lambda=-\frac{\pi}{2}$, the solution is given by the same expressions as (14) and (15) except replacing v_0 by $-v_0$. The distributions of temperature and of coefficient β with height are shown in Table 2. The velocity adopted is 5 m/s. In this calculation it is supposed that the production maximum of the electron lies at 270 km in summer (χ is smallest) and at 370 km in winter. The electron drifts downwards in winter and upwards in summer. It is not evident whether or not this assumption agrees with the real condition, but the effect of the temperature will be verified. Figs. 8 and 9 show the results of calculations. The static regions in two

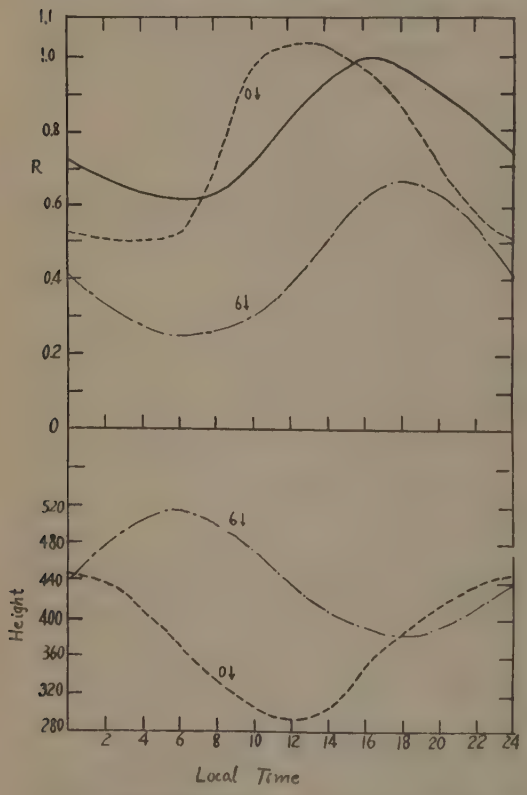

Fig. 8 Daily variation of electron density and height of moving region with uniform velocity when temperature increases linearly with height. Full line represnts static region.

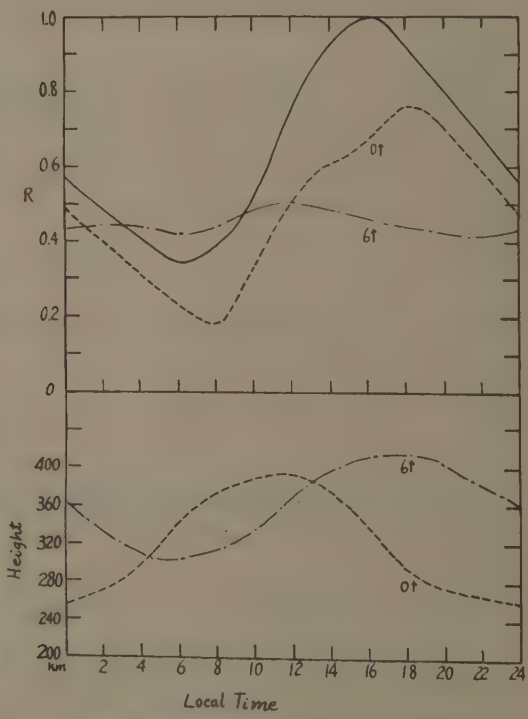

Fig. 9 Daily variations of electron density and height of moving region with uniform velocity when temperature increases linearly with height. Full line represents the static region.

figures represented by the full lie are respectively similar with those in Fig. 6 and 7, and the maximum density of the day is 3.9 $\times 10^4 q_0$ and $2.3 \times 10^4 q_0$. The daily variation of the electron density in Fig 8 for 0↓ shows the great increase compared with the corresponding curve in Fig. 6. On the other hand, the variation of 6↑, 0↑, shows the decrease relative to the static region than the corresponding curves in Fig 7, especially, the decrease for 6↑ reaches 50%. The variation of height is analogus to those in Fig 6 and 7.

Table 2

Height	Temperature	Attachment Coeff.
400km	2200°k	1×10^{-5}/s
380	2000	1.15×10^{-5}
360	1800	1.25×10^{-5}
340	1600	1.35×10^{-5}
320	1400	1.5×10^{-5}
300	1200	1.8×10^{-5}
280	1000	2.2×10^{-5}
260	800	2.9×10^{-5}
240	600	3.9×10^{-5}
220	400	6.0×10^{-5}
200	400	1.0×10^{-4}

7. Explanation of Daily and Seasonal Anomalies of Electron Density and Height

General aspects of variations of f_0F2 and $h'F2$ are shown in Fig. 10. Since the variations of f_0F2 and h_pF2 (analogaus to $h'F2$) in winter in northern hemisphere are analogous to those in summer in the southern and the reverse case also holds, we hereafter disccuss the variations in the northern hemisphere.

(i) We first investigate whether the daily variations in two solstices can be explained by the vertical drift. We consider that the effect of the semi-diurnal

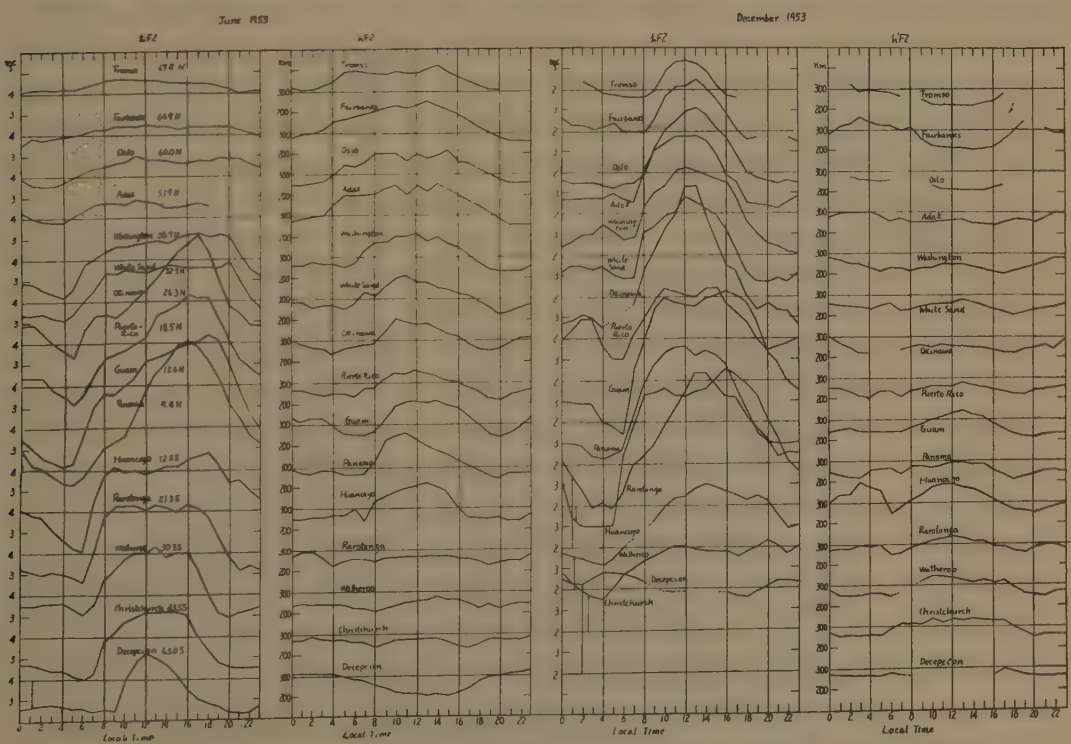

Fig. 10 Daily variations of f_0F2 and $h'F2$ in various latitudes in Jun. and Dec. 1953.

drift is small. As shown in § 5 and § 6, including the effect of the temperature gradient with height, the decrease of the electron density relative to that of the static region (no drift) is about 20% for the diurnal drift of 0↑ which is considered to occur in summer and about 50% for the drift of 6↑ which is cosidered to occur near magnetic equator, while for the drift of 0↓ which corresponds to the case in winter, the daily variation is considered to be almost equal to the static case. In equinox the drift is mainly of semi-diurnal and drift of 0↓ adds in high latitudes. So that in equinox the daily variation is approximately the same as the static region. But in this season the anomaly in electron density exists. This reason is inferred in (v) of this section. In winter since the daily variation, save the case of low latitude, is regarded as that of the static region, the observed variation will be obtained, provided that the attachment coefficient in the region of electron production is 3×10^{-5}/s–5×10^{-5}/s based on the estimation shown in § 8. On the other hand, in low latitudes throughout the year and above the middle latitudes in summer, the data indicate that an upward drift influences on the electron density and height. In § 2 we showed that near the magnetic equator the electron density is reduced by about 50% from the static Chapman norm. This is understood easily if we consider that there is an electron drift of 6↑. If this drift is present throughout the year, the trough in magnetic equator is always set up. Hirono and Maeda [20] also indicated that the vertical electron drift of 7.3^{h}↑ leads to an observed daily variation at Huancayo, and the reduction of the electron density from the static Chapman norm is abont is 40%–60%. Their method of integration of the equation of continuity is numerical and the decay of the electron is of a recombination type. Our calculation differs more or less from those by them, but the results are well consistent with theirs. Now the summer daily variation of electron density become smaller for higher latitude, and the ratio of density at sunrise to the maximum of the day is 1/1.5–1/3, while 1/10–1/15 in winter. This makes us to regard that the static region in summer lies at the level of smaller value of β than that in winter. But in all our calculations the sunshine begins at $06^{h}\,00^{m}$ and sunset at $18^{h}\,00^{m}$. In reality the time of sunrise approaches more to midnight as the latitude becomes higher, the duration of the sunshine, therefore, longer and the variation of the intensity of the radiation smaller. Under these conditions the daily variation of the electron density becomes smaller. As an extreme case we regard the sun shines all over the day with a constant intensity. Then the solution of $\frac{\partial N}{\partial t}=q_0-\beta N$ is $\frac{q_0}{\beta}$ which implies a constant electron density. This characteristic makes β to be small apparently. If this characteristic and the influence of the vertical electron drift of 0↑ are taken into consideration the summer daily variation of the density above middle latitude can be explained when the attachment law is applied as the electron decay. If the decay of the electron is recombination type, we cannot help but consider that the production of the electron in summer is higher than in winter. The height variation is accounted for by vertical drift.

(ii) Let the static region lies at the height respectively 4×10^{-5}/s and 6×10^{-5}/s in winter (w) and summer (s) about 30° in latitude (reason described in § 8). Then the ratio $\left(\frac{N_s}{N_w}\right)$ of the electron density at noon in two solstices is $\frac{N_s}{N_w}\simeq\frac{1}{1.5}\frac{q_s}{q_w}$, where q is the electron production at noon. This estimation is based on the daily variation mentioned in (i). If the electron is proportional to $\cos\chi$, $N_w\simeq N_s$ is obtained. At 50°, $\frac{N_s}{N_w}\simeq\frac{1}{2}\frac{q_s}{q_w}$, and since $q_s\simeq3q_w$, $N_w<N_s$ is obtained. Thus the seasonal anomaly of the electron density in such latitudes does not occur. Nevertheless, in reality, anomaly takes place. If we take Bradbury's hypothesis, the maximum of the electron density in the $F2$ region lies higher by two or more in scale height than that of the $F1$ region. If we take two in scale height, $N_s\simeq1.2N_w$ at 50°, If distance of two maximum is more than two in scale height, the possibility $N_s\simeq N_w$ is present. So that, a part of the seasonal anomaly is in this case explained. In consquence, the anomalous seasonal variation cannot be accounted for only by the vertical drift.

(iii) There are other facts which can not be explained by the vertical drift only. They are:

(a) Increase of electron density from s.s. min to s.s. max. is greater in writer than in summer and the seasonal anomaly of electron density is amplified worldwidely during s.s. max. far more than s.s. min. as shown in Fig. 3. This amplification therefore becomes larger for higher latitude.

(b) There is an increase of h_pF2 during s.s. max. compared with that during s.s. min..

(c) The latitudinal distribution of f_0F2 even in equinox is better in geographic than in geomagnetic above 30° and a slight seasonal anomaly still exists.

(d) h_pF2 in winter does not incsease in higher latitudes and rather decreases.

(e) Distribution of f_0F2 in low latitude against $\cos\chi$ deviates from the line $f_0F2\propto\cos^{\frac{1}{2}}\chi$. The greater the sunspot number, the greater this deviation.

(f) There are many stations where $h'F1$ in summer is larger than that in winter or at least equal, as shown in Fig. 11. This is the reverse to Chapma's law. On the other hand, daily variations of $h'F2$ and f_0F1 obey well his law.

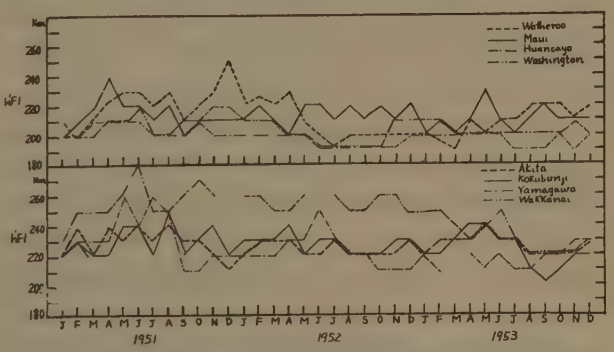

Fig. 11 Seasonal variation of noon median value of $h'F1$ from Jan. 1951 to Dec. 1953.

It is necessary to add brief comments. First to (a) and (b), we first considered that both the amplification of anomaly of election density and the increase of h_pF2 are due to the augumentation of the vertical drift. Since it is likely that the variation of h_pF2 represents a direct result of the drift, the daily variations of h_pF2 at Kokubunji, Washington and several other stations during s.s. max. and s.s. min.

are put in a harmonic analysis. The result shows that only the constant term (mean level) incseases and no appseciable increase of diurnal and semi-diuanal components takes place. To (c), it is known from a harmonic analysis of the height that there is no appreciable effect of the diunal drift in equinox. Hence the slight anomaly is probably due to the cause associated with the geographic latitude. Finally to (f), we consider that the behaviour of $h'F1$ in summer is due to an elevation of the production, because in such a height β is very large and the electron drift is remarkably reduced.

At any rate in (ii) and (iii) we described that the variation of h_pF2 and f_0F2, including the seasonal anomaly, cannot be accounted for only, by the geomagnetic effct unless other geographical or solar factors are taken into consideration. It is the next problem to study what this factor is.

(iv) That the seasonal variation of electron density may be explained by both the vertical electron drift and the variation of the temperature, was suggested by Wiss [21]. We briefly touch this. It is considered that the temperature variation acceptable physically is very small [5]. If the temperature is expressed by (12) the production of the electron is given by

$$q=An_0\delta S_\infty\left(\frac{T}{T_0}\right)^{-\left(1+\frac{l}{\gamma}\right)}\exp\left[-An_0T_0l^{-1}\sec\chi\left(\frac{T}{T_0}\right)^{-\frac{l}{\gamma}}\right],$$

$$l=\frac{mg}{k}, \tag{16}$$

where A, S_∞, m, g, and k represent respectively the absorption coefficient of the par ticle, the total solar flux at the top of the atmosphere, the mass of the particle, the gravitational constant and Boltzmann's constant. n_0 and T_0 represent respectiveley the particle number and the temperature at the reference level. The maximum production of electron (q_m) is given by

$$q_m=An_1\delta S_\infty\exp\left[-\left(1+\frac{\gamma}{l}\right)\right], \tag{17}$$

with

$$An_1T_1\sec\chi=l+\gamma, \tag{18}$$

where n_1 and T_1 represent respectively the number density of the particle and the temperature at the level of q_m. The ratio of q_m in summer to that in winter is given by

$$\frac{(q_m)_s}{(q_m)_w}=\frac{\cos\chi_s(l+\gamma)_se^{-\left(1+\frac{\gamma}{l}\right)_s}}{\cos\chi_w(l+\gamma)_we^{-\left(1+\frac{\gamma}{l}\right)_w}}\frac{T_{1w}}{T_{1s}}, \tag{19}$$

where suffixes refer to the summer and winter. The value of l is 33.1×10^{-5}K/cm 16.5×10^{-5}K/cm and 18.8×10^{-5}K/cm for nitrogen molectule, nitrogen atom and oxygen atom. Since γ may be much less than (probably 3×10^{-5}K/cm–5×10^{-5}K/cm) there still be $(q_m)_s>(q_m)_w$ by a factor of 1.5 or 2.0 in middle latitudes even if in summer γ becomes twice that in winter. Hence the decrease of q_m resulting from the increase of temparature is small.

Next the daily variation of the electron density due to variation of the temperature without the electron drift, is given by

$$\frac{\partial N}{\partial t}=q-\beta N-\frac{N}{T}\frac{\partial T}{\partial t}=q-\left(\beta+\frac{1}{T}\frac{\partial T}{\partial t}\right)N. \tag{20}$$

We assume the daytime departure of temperature from the mean (the value at 06^h00^m) is 10%, then T in the bracket in right side of (20) may be taken to be constant. If the temperature varies as follows

$$T=T_0+T_1\sin\omega t, \tag{21}$$

then

$$\frac{\partial T}{\partial t}=T_1\omega\cdot\cos\omega t.$$

Since $T_1/T_0=1/10$, $\frac{1}{T}\frac{\partial T}{\partial t}\simeq 7.3\times10^{-6}$/s at 06^h00^m and $\frac{1}{T}\frac{\partial T}{\partial t}=0$ at noon. Hence $\frac{1}{T}\frac{\partial T}{\partial t}$ is less than β. Thus the solution of (20) is not much different from that of the equation without the tempererature term. In consequence the temperature variation physically acceptable gives little influences on the electron density.

(v) It appears that the difficulty in (ii) and the phenomena in (iii) in this section cannot be accounted for by combining effect of both vertical electron drift and the temperature variation. In order to explain these matters simultaneously, the following is suggested. That is, there must be a seasonal variation of the height distribution of the particle responsible for the $F2$ region. For example, we presume that various kinds of particle distribute with the common scale height, in other words, they are in a mixing state, when the sun is overhead, (for large $\cos\chi$) and on the other hand, they are probably in a diffusive equilibrium state with different scale height one another for small $\cos\chi$. The distribution variation of the particle is due to the deeper penetration of the solar radiation into the atmosphere for large $\cos\chi$. In winter the particle distributes in a diffusive equilibrium in high latitude and in summer the partcle approaches to the mixing state. Thus the variations of the distribution is larger for higher latitude. In low latitude, including the equatorial zone, the sun is always overhead and hence particles are always in a mixing state, though the state may be not the same as that in summer in middle latitude. The distribution variation in the $F2$ region takes place also when the original variation of distribution is present below the $F2$ region (e.g. near the E region). If the $F2$ region is formed by ionization of the particle which increases its number density at certain heights when the distribution varies, the phenomena mentioned in (ii) and (iii) are easily accounted for. The reason is as follows. If the particle distributes in the atmosphere where the scale height in creases linearly with the height gradient α, the maximum electron production is representedd by

$$q_m=An_1\delta S_\infty\exp[-(1+\alpha)], \tag{22}$$

with

$$An_1H_1\sec\chi=1+\alpha. \tag{23}$$

In certain latitudes we suppose that S_∞, α, δ, χ, A are all constant. Then the height of q_m depends on the product n_1H_1 and its magnitude depends on n_1, the number density at the level of the maximum production. If the number density of the particle at certain level incraeses which means the increase of scale height

(and o), when the atmospheric state changes from the diffusive equilibrium to the mixing, the level of the maximum production of the electron rises ((iii) in § 8) and the number of the electron production is reduced due to the decrease of n_1 accompanying increase of H_1 as seen in (23). Since H_1 depends on the mass of the particle and the temperature, a fairly large reduction of q_m from that in the normal diffusive state, about by a factor of 2–4, is expected in summer. So that the anomalous seasonal variation of f_0F2 may be accounted for.

Now if the elevation of the maximum production is possible owing to the variation of the distribution of the particle, (d) in (ii) is easily accounted for, because in winter the distribution approaches the diffusive equilibrium state more and more as the latitude increases and the number density at the same height becomes smaller. Since the electron production decreases much more in lower latitude, compared with that in a diffusive epuilibrium, electron density decreases and deviates from the line of $f_0F2 \propto \cos^{\frac{1}{2}}\chi$. Thus (e) is explained. If this variation of distribution also present in the $F1$ region also (f) is possible. If during s.s. max. the change of the distribution to the mxing state is more promoted than during s.s. min. both reduction of the electron production at maximum level and the elevation of its level will be amplified. Thus (a), (b) and (e), are explained. In the equatorial zone below 20° there is little change of the distribution of the particle so that variation of seasonal electron density obeys to such a way as that of the E and $F1$ region. This is consistent with the observed data.

In consequence, it appears that there are two main causes for the variation (including so-called anomalies) of f_0F2 and h_pF2. One is the geomagnetic distortion which is brought by the vertical electron drift and the other the geographic effect which is here considered as variation of the distribution of the particle responsible for the $F2$ region. The former is predominant near the magnetic equator, and the latter, in middle and high latitudes. Hence near the equator, the electron density is decreased even by a factor of 4–6 during s.s. max., compared with that in the case of no mixing and no drift. (see Fig. 2)

8. Discussions

(i) It is a very important question whether the solar diurnal and semi-diurnal drift are present in the $F2$ region. The lunar and solar semi-diurnal drifts have already been discussed by Martyn. Hirono [22] also calculated the lunar semi-diurnal drift, taking the anisotropic conductivity of the ionosphere into consideration. According to him, the phase of the drift is constant from pole to equator over two hemispheres, and he predicted that in the solar semi-diurnal drift the relationship of the phase with latitude is closely similar to that of lunar case. This result coinsides with that concerning the phase shown in § 3. As to the solar diurnal drift the cause has not yet been known. But the presumption from the fact that there are the diurnal and semi-dirnal components in the S_r variation of the earth's magnetic field, in which the former is larger than the latter, leads to the presence of an electric current system responsible for the diurnal component. It

is considered that there may be an electric current (or electric field) in the $F2$ region, which is associated with the above current system, and such a observed diurnal drift is set up. If the electric field which is estimated from the S_q variation is present in the $F2$ region in magnetic equator, upward drift in daytime throughout the year is set up. [20].

As one of the casuses of the drift, it is expected that the electron moves along the magnetic line of force of the earth owing to the diunal wind which varies with season. For this purpose, the wind which blows from north to south in summer and opposite in winter in the northern hemisphere is necessary. However, Briggs and Spencer [23] indicated that many observations in the world show the reverse winds respectively in summer and winter to that which we need. Hence the direct drift of the electron due to the wind is not consistent with the present observed data.

(ii) The latitudinal distribution of f_0F2 in Dec. shows that it obeys the law of $f_0F2 \propto \cos^{\frac{1}{2}}\chi$. We inferred from this fact that the decay law of the electron is of an attachment type. Morever in § 7 it is found that decay of the electron by the attachment law is appropriate to account for the daily variation of f_0F2. Besides these, there is another important phenomenon in favour of the attachment law ; i.e., the rate of the increase of electron density in the $F2$ region from s.s. max. to s.s. min. differs from that of the $F1$ region. This difference is removed if the decay law in the $F2$ region is of the attachment type while that in the $F1$ region is of recombination type. Further evidences to adopt the attchment law were shown by Yonezawa [24]. So that it seems that the attachment law should be applied to the $F2$ region.

We can presume the magnitude of β in the $F2$ region in winter in the following ways.

(a) The variation of $h'F2$ in winter shows the conspicuous semi-diurnal variation. This implies that variation of the height is not at all due to the penetration of the solar radiation only, but the semi-diurnal drift influences on the height variation. In order to permit the effect of the drift β should be less than 10^{-4}/s.

(b) The time lag of the maximum density of the day from the noon is about 3 hours for 2.7×10^{-5}/s. To get the observed time lag β will be 5×10^{-5}/s-7×10^{-5}/s.

(c) The ratio of the electron density at sunrise to the maximum of the day is about 1/10–1/15 (observed value). According to our calculation this ratio is obtained if $\beta=3\times10^{-5}$/s–5×10^{-5}/s.

(d) The magnitude of the electron production is about 80/cc/s for 2.7×10^{-5}/s when the maximum electron denity is taken as 1.5×10^{6}/cc. If the production has the value near to this, $\beta=3\times10^{-5}$/s–5×10^{-5}/s is hopeful.

From these points of view, the value of β in the $F2$ region in winter may be 3×10^{-5}/s–5×10^{-5}/s and the height corresponding to this value may be 250km–300km.

(iii) We suggested a seasonal variation of the number density of the particle at any height in the $F2$ region. Nicolet and Mange [25] indicated that there may

be a downward movement of particles in the $F2$ region, in relation with the downward movement of the oxygen atom in the lower ionosphere near the E region. The diffusive separation may take place at about 160 km level ([25], [26], [27]). Hence there may be possible that the particle which contributes to the $F2$ region, distributed in diffusive equilibrium in winter, changes its distribution owing to the mixing in summer and increases the number density at a certain level of the electron production.

Above the height of 200 km the main particles are probably O, N_2 and N. For example we assume that the $F2$ region is attributed to the ionization of N_2 and this particle distributes in a diffusive equilibrium state from the height of 160 km in winter. Let the temperature at this height be 430°K and above that height the temperature increases linearly with the gradient of 3°K/km, then in summer, owing to the transition to the mixing state, O and N, which is considered to be present above 200 km [28], move downwards and in turn, N_2 upwards. Thus the number density of N_2 may increases by a factor of 5–8 at 250 km. So that the level of maximum production rises higher than one scale height. If the particle responsible for the $F2$ region is O, this phenomenon is reversed. In the case of N, its variation of number density is very complicated because the dissociation of N_2 must be taken into consideration.

9. Conclusion

It is found that the anomalous variations in the $F2$ region are ascribed both to geomagnetic and to geographic causes. Of anomalies, the trough in magnetic equator can be satisfactorilly accounted for by the diurnal electron drift. The reason for geographic control of f_0F2 in writer is also described. Other variations, i.e. seasonal variations of f_0F2 and several behaviours of h_pF2 and f_0F2 pointed out newly are explained if we assume that the height distribution of particle varies seasonaly.

Acknowledgement

The author wishes to express his thanks to Prof. M. Hasegawa of Geophysical Institute, Kyoto University, for his kind advice and to Prof. K. Maeda of Institute of Electrical Engineering, Kyoto University, for valuable discussion in the course of this study.

References

[1] S. Chapman, Proc. Roy. Soc., A, **43**, 26 (1931)
[2] E.O. Hulburt, Phy. Rev., **46**, 822 (1934)
[3] D. Lepechinsky, J. Atmosph. Terr. Phy., **1**, 278 (1951)
[4] J.A. Gredhill, and M.E. Szendrei, Proc. Phys. Soc., B, **63**, 427 (1950)
[5] D.F. Martyn and O.O. Pulley, Proc. Roy. Soc., A, **154**, 455 (1936)
[6] V.C.A. Ferraro, Terr. Mag., **50**, 215 (1945); **51**, 427 (1946)

[7] D.F. Martyn, Proc. Roy. Soc., A, **189**, 241 (1947); **190**, 273 (1947); **194**, 429 (1948); **194**, 445 (1948)
[8] A.A. Weiss, J. Atmosph. Terr. Phys., **3**, 30 (1953)
[9] K. Maeda, Rep. Ionos. Resear, Japan, **7**, 81 (1953)
[10] T. Shimazaki, J. Rad. Resear. Lab., in press
[11] E.V. Appleton, Nature, **157**, 691 (1946)
[12] H.L. Lung, J. Geophys. Resear., **54**, 177 (1949)
[13] Y. Aono, Rep. Ionos. Resear. Japan, **7**, 30 (1953)
[14] K. Maeda, Rep. Ionos. Resear. Japan, **8**, 155 (1953)
[15] S. Chapman, Proc. Phys. Soc., **43**, 483 (1931)
[16] N.E. Bradbury, Terr. Meg., **43**, 55 (1938)
[17] T. Sato and T. Namikawa, J. Geomag. Geoelectr., **6**, 157 (1954)
[18] A.P. Mitra, J. Atmosph. Terr. Phys., **1**, 286 (1951)
[19] D.R. Bates, Proc. Roy. Soc., A, **196**, 562 (1949)
[20] M. Hirono and H. Maeda, J. Geomag. Geoelectr. **6**, 127 (1954)
[21] A.A. Weiss, Austr. J. Phys., **6**, 291 (1953)
[22] M. Hirono, J. Geomag. Geoelectr., **5**, 22 (1953)
[23] B.H. Briggs and M. Spencer, Prog. Phys., **17**, 245 (1954), (Proc. Phys. Soc.)
[24] T. Yonezawa, Rep. Ionos. Resear. Japan, 8 64 (1954)
[25] M. Nicolet and P. Mange., J. Geopys. Resear., **59**, 15 (1954)
[26] A.P. Mitra, Private Communication.
[27] H. Lettau, Compendium of Meteorology, 320 (1951), Ed. T.F. Malone, Amer. Met. Soc.
[28] T. Sato, J. Geomag. Geoelectr., **5**, 71 (1953)

Studies on the Disturbances in $F2$ Layer Associated with Geomagnetic Disturbances*

By Kenzi SINNO

Hiraiso Radio Wave Observatory, Radio Research Laboratories, Japan.

Abstract

The existence of some correlation between the geomagnetic storm and the ionospheric $F2$ layer disturbance has long been investigated since the early stages of ionospheric researches. Recenty, this problem has been studied by many investigators not only from geophysical interest but also under the necessity of improving radio communications.

The main course of investigation on $F2$ disturbance, which has been studied by the author for the last three years, is summarized as follows:

(1) The separation of variations in f^0F2 and $h'F2$ associated with geomagnetic storms into two parts depending on the universal time and local time, the so-called $Dst(F2)$ and $S_D(F2)$, respectively, was clarified.

(2) The devlopment process of the $F2$ disturbance was investigated in respect to each of $D_{st}(F2)$ and $S_D(F2)$. It is concluded that $S_D(f^0F2)$ exists in the earlier stage of geomagnetic storm and $D_{st}(f^0F2)$ grows in the comparatively later stage.

(3) The latitudinal and seasonal characteristics were shown.

(4) Investigations were made in the behaviour of the $F2$ layer according to the different levels of geomagnetic activities. Results showed that the $F2$ layer disturbance was generally in proportion to the geomagnetic activities, except for $D_{st}(f^0F2)$ variation in winter.

(5) As to the successive yearly variation of ionospheric disturbance, it was found that the phase of $S_D(F2)$ would lag behind according to the decrease of sunspot activity.

1. Introduction

The existence of irregular variations in the $F2$-layer associated with geomagnetic disturbances had been investigated in the ealier stages of ionspheric researches by E. V. Appleton, etc. [1] and L. V. Berkner, etc. [2] By gradual steps,

* Previous reports (3) (4) and (5) on investigations by the author are collected in this paper.

the morphology of ionosphere disturbance was being clarified, but these investigations were intermitted by World War II until some four years ago. Recently, this problem has been studied by many investigators [3] from both geophysical interest and practical necessity.

The first step to do was the statistical separaiton of variations in f^0F2 and $h'F2$ into parts depending on the storm and local time (longitude), respectivly, as was done in the case of variations in geomagnetic forces during geomagnetic disturbances.

After this was done, the morphology of $F2$ disturbance was clarified without difficulty and some foundation was laid for the warning of radiocommunication disturbance.

2. Separation of $F2$ Disturbance into $D_{st}(F2)$ and $S_D(F2)$

The success of separation into D_{st} and S_D parts of the geomagnetic variation suggests the same success in the case of $F2$ disturbance because of close interrelationship existing between them. Under this consideration, we are applying the same method to the ionospheric data in this paper.

As the ionospheric quantities there are taken the values of $\frac{\Delta f^0F2}{f^0F2*}$ (where Δf^0F2 represents the deviation of f^0F2 from the monthly median value, and f^0F2* represents the monthly median value) and $\Delta h'F2$ for many stations in different seasons.

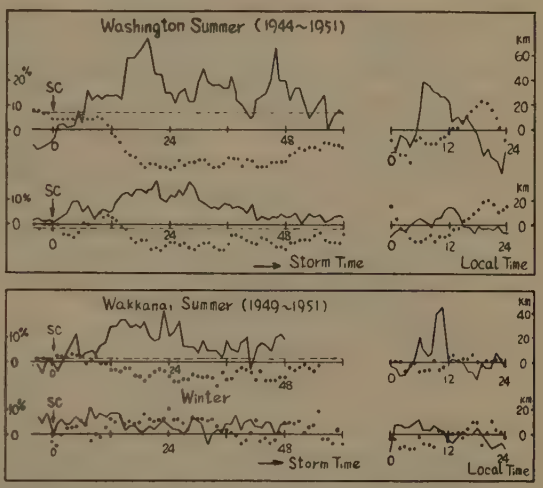

Fig. 1 D_{st} (left) and S_D (right) parts of the $F2$ disturbance at Washington and Wakkanai. Variations in $\frac{\Delta f_0F2}{f_0F2*}$ by dotts and $\Delta h'F2$ by lines.

As shown in Fig. 1 quoted from my earlier report [4], we can easily find that the $F2$ variation contains two variable parts like D_{st} and S_D during the magnetic storm.

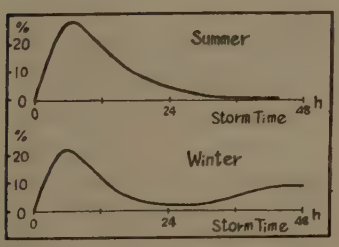

Fg. 2 Development of the amplitude of $S_D(f^0F2)$ at Washington (1944~51).

3. Characteristics of $F2$ Disturbance

3. 1. *Developing process of F2 disturbance*

The development of the $D_{st}(F2)$ part is shown in Fig. 1. As shown in Fig. 3, D_{st} disturbance of $h'F2$ begins gradually without delay after *SC* in spite of the fact that f^0F2 variation has not an appreciable change immediately, and then large variation follows 8~10 hours after *SC*. This fact shows that the ionospheric disturbance is not of

propagation phenomenon from high latitude toward low latitude, but it begins simultaneously with *SC*.

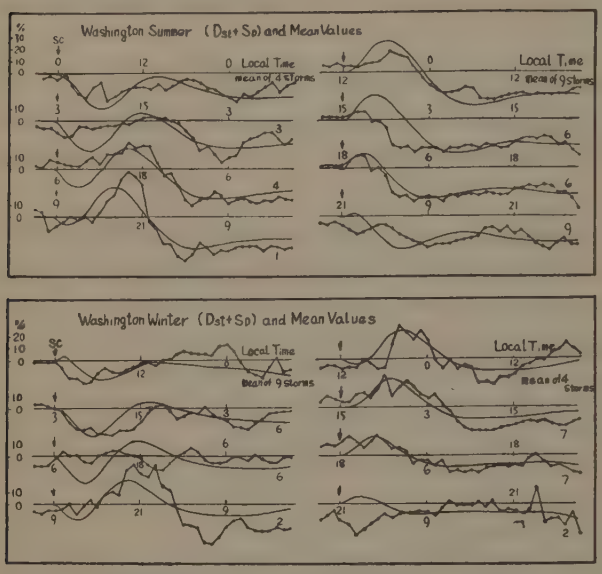

Fig. 3 Development of $F2$ disturbances in f^0F2 at Washington (1944～51), having their sudden commencement at different local times.

The development of the $S_D(F2)$ part is shown, under the approximation of the sine curve, in Fig. 2 at Washington (1944～51) as described in the previous report [5]. By combining Fig. 1 and Fig. 2 we can reproduce the original disturbances which have begun with *SC* occurring at different local times as shown in Fig. 3.

On the other hand, in order to study the development of $S_D(F2)$, without assuming the constant phase, we can use the storm time diagram of f^0F2. This was done for Washington f^0F2 [3] in summer and winter, as shown in Fig. 4.

We can see that $D_{st}(F2)$ begins with a large change at about 8～10 hours and the maximum amplitude of S_D occurs 6～12 hours after *SC*. Then it is found that S_D is large in the early stage of the magnetic storm, but D_{st} predominates later on. It seems that the latter has not so good flexibility as the former according to the magnetic variation. As seen in Fig. 4, the phase lag of S_D is clear especially at the last phase of the disturbance. This fact was also pointed out by Mr. T. Obayashi [3] in his study of individual behaviour of $F2$ disturbance.

The above development processs of $F2$ disturbance will be helpful to the prediction of radio communiction disturabnce. For instance, Fig. 3 may serve as an important key to forecast the world-wide distribution and development of disturbance in regions in which is measured the lower field intensity of radio waves.

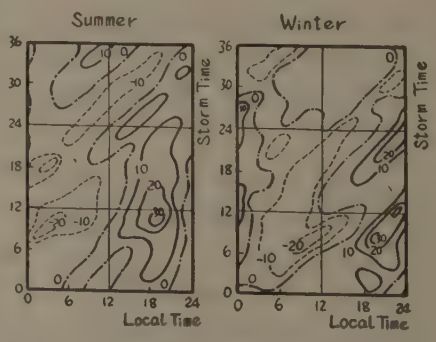

Fig. 4 Storm-local time diagram fo S_D (f^0F2) at Washington (1944～51) in summer and winter.

3.2. *Latitudinal and seasonel characteristics of F2 disturbance*

a. Latitudinal characteristics

The data used concern f^0F2 observed at Fraserburgh, Washington, Wakkanai, Yamagawa, Huancayo, Singapore, Brisbane, Falkland Island, Hobert and Macquarie Island, during the summers and winters of

from 1949 to 1951 (Fig.5).

The results are expressed in geomagnetic latitude local-time diagrams of $S_D(f^0F2)$ and geomagnetic latitude-$Dst(f^0F2)$ diagrams, as are shown in Fig. 6 (a) and (b). Here, $\overline{D_{st}}(f^0F2)$ are the mean values of $D_{st}(f^0F2)$ during the period of 48 hours subsequent to *SC* in the stormy time.

In this figure is shown that the phase of $S_D(f^0F2)$ lags from summer to winter hemisphere. It is strange that this phase changes gradually to about 180° without an equatorial node. $\overline{D_{st}}(f^0F2)$ illustrates the well-known fact of the summer decrease and winter increase in f^0F2 with the exception of the singular area of $\overline{D_{st}}(f^0F2)$ which exist at about 50° geomagnetic latitudes as shown Fig. 6.

b. Seasonal characteristics

As are shown in Figs. 5 and 6, the $D_{st}(f^0F2)$ variation has a general tendency to decrease in summer and increase in

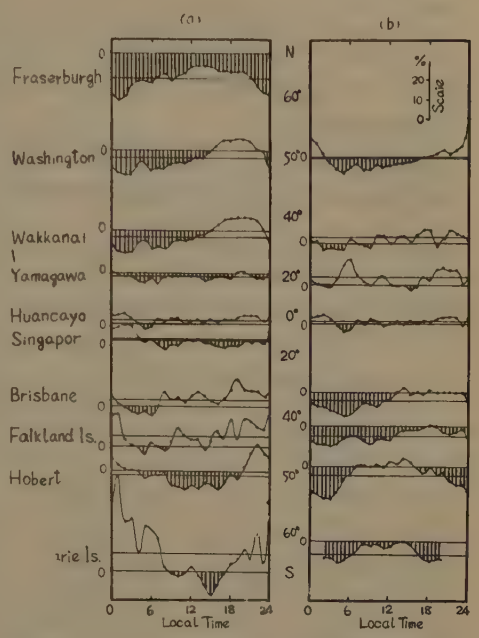

Fig. 5 (a), (b).$F2$ disturbances of f^0F2. When the northern hemisphere is in summer (a) and in winter (b). Shaded areas indicate the negative values of $S_D(f^0F2)$.

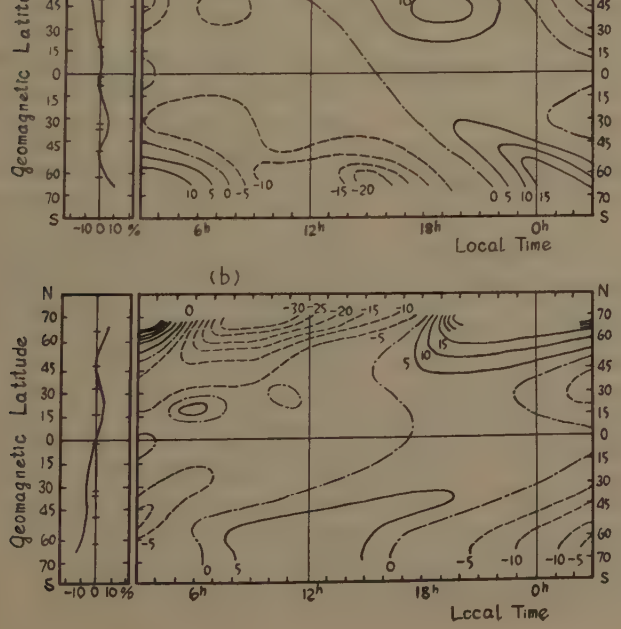

Fig. 6 (a), (b). Both (a) and (b) show f^0F2 disturbances in percentage with respect to geomagnetic latitude and local time, in different solstitial seasons, respectively, as described in Fig. 5. The left show Dst part, and the right S_D part, both being thea verages of 48 hours in stormy time.

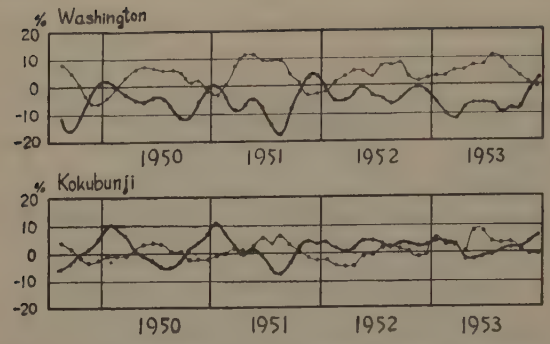

Fig. 7 The average of 24 hourly mean values of $\frac{\Delta f^0F2}{f^0F2^*}$ on the five international monthly geomagnetically disturbed days and quiet days at Washington and Kokubunji. Thick lines are for disturbed days and thin lines for qniet days.

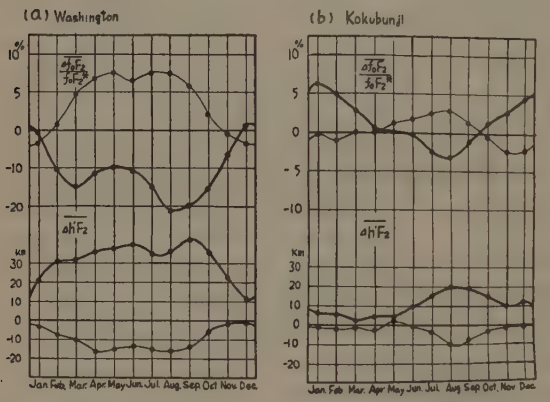

Fig. 8 (a), (b).
Average seasonal characteristics of $D_{st}(F2)$.

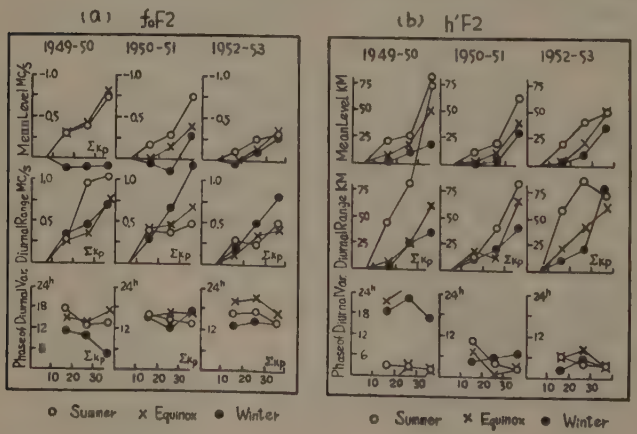

Fig. 9 (a), (b).
Deviations of f^0F2 and $h'F2$ at different degrees of activities from the groups of the calmest magnetic activity, are summarized in three principal quantities: the magnitude of D_{st}, S_D and the phase of S_D, respectively.

winter.

Fig. 7 shows the average of 24 hourly mean values of $\frac{\Delta f^0F2}{f^0F2^*}$ on the five international monthy geomagnetically disturbed days and quiet days both at Washington and Kokubunji. From this figure, we can see the seasonal and yearly variation of $D_{st}(f^0F2)$, but the latter does not well appear, particularly at Washington, owing to the values divided by median values.

The average curves of D_{st} (f^0F2) for about 4 years from July, 1949, to February, 1954, and $D_{st}(h'F2)$ for about 2 years in the same period are shown in Fig. 8 (a) and (b). The tendency that $h'F2$ is elevated on geomagnetically disturbed days and is depressed on quiet days is witnessed in common at both stations. It is noticeable, however, that the curves of disturbance days in f^0F2 have two minima near the equinoxes and the curves of quiet days have two maxima, and both curves are mirror images of each other. These maxima and minima are not attributed to the equinoctially maximum activities of geomagnetism, for the reason stated in the following subsection. Hence, it may be considered that Fig. 8 expresses the seasonal tendency of the ionospheric disturbing sensibility.

3.3. *On relations between the grade of geomagnetic activity and F2 disturbance*

The ionospheric variations are investigated on the basis of the data of Washington over the years 1949～1953 divided into three groups of the year.

The geomagnetic activities are expressed by ΣKp, which is the summation of Kp's of the whole day. The corresponding $F2$ values used here are the deviations of the mean values of $f^0F2(h'F2)$ which belong to the groups of days of $13\text{-} \leqq \Sigma Kp \leqq 22 \leqq +$, $23\text{-} \leqq \Sigma Kp \leqq 32+$ and $\Sigma Kp \geqq 33\text{-}$, from the values belonging to the quietest group $\Sigma Kp \leqq 12+$.

In order to show the principal characteristics of these deviations, noncyclic variations [6] are subtracted from the above deviations and they are smoothed by means of three hourly running averages. The three main characteristics, that is, the mean values over 24 hours, the range of diurnal variations, and the centre time between the times of maximum and minimum values of the curves, for each group of days in the three seasons, respectively, are summerized in Fig. 9 (a) and (b), and an example of the original curves f^0F2 in case of $\Sigma Kp \geqq 33\text{-}$ is shown in Fig. 10.

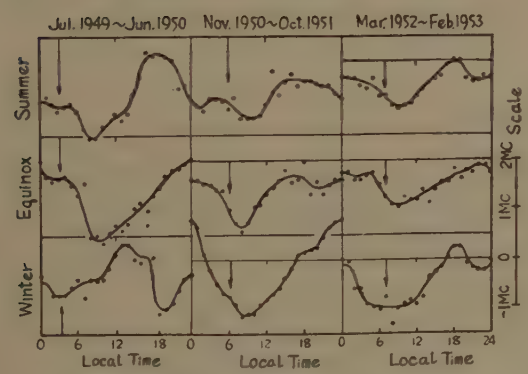

Fig. 10 Example of the original curves in f^0F2 corresponding to the case of $Kp \geqq 33\text{-}$.

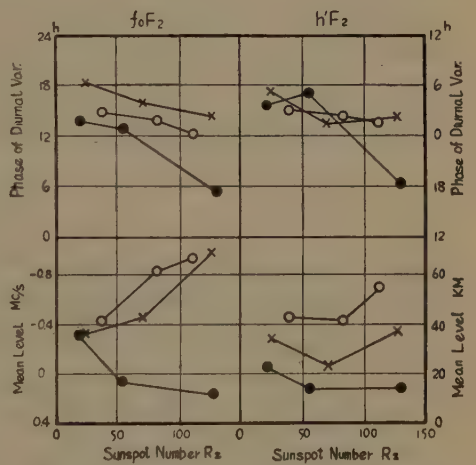

Fig. 11 Variation of the phase of S_D and the level of D_{st} at Washington according to the sunspot number R_Z in different seasons.

Fig. 9 shows that $F2$ layer is generally disturbed in proportion to the geomagnetic activity except for the $D_{st}(f^0F2)$ variation in winter.

At Akita and Brisbane, these former characteristics are also accepted.

3.4. *Yearly characteristics of F2 disturbance*

For using $\frac{\Delta f^0F2}{f^0F2^*}$ which is divided by the monthly median valus as shown in Figs. 7 and 9, the yearly variation of $F2$ disturbance is not remarkable in the amplitude of seasonal variation as described above, but Δf^0F2 is conspicuous by its successive yearly variation in proportion to the solar activity.

The same character exists as well in $S_D(f^0F2)$, and additionally S_D has a tendency to advancement of the phase according to solar activities. (Fig. 11)

In summer and equinoctial seasons, the variations of $f^0F2(h'F2)$ decrease (increase) continuously as geomagnetic activities increase. In winter, however, the behaviour of $F2$ layer is not so simple, for f^0F2 rises from slight to moderate magnetic activity and $h'F2$ monotonously increases as illustrated in Fig. 12. This behaviour is considered to be the general nature of the disturbance in winter, as was discovered by L. V. Berkner, [2] etc. at Wathroo during the epoch of the larger sunspot number.

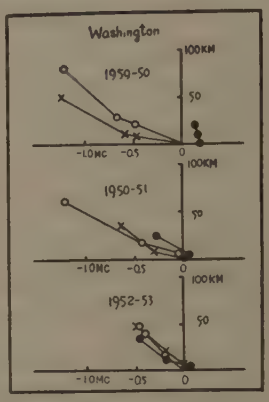

Fig. 12 Diagrams of $D_{st}(f^0F2)$ and $D_{st}(h'F2)$.

4. Concluding Remarks

The above characteristics of the $F2$ disturbance associated with geomagnetic disturbances are recognized, without any remarkable contradiction, by other investigators somewhat different methods and data. There will be some time before the complete morphology of $F2$ disturbance is accomplished. And yet on this ground will be founded the theory of ionospheric disturbance and the prediction of radio disturbance. In closing, the writer wishess to express his sincere thanks to Dr. H. Uyeda and Prof. T. Nagata for their continued interest and encouragement given him throughout this work.

References

[1] E. V. Appleton and L. J. Ingram, Nature, **136,** 548 (1935).
[2] L. V. Berkner, H. W. Wells and S. L. Seaton, Terr. Mag., **44,** 238 (1939).
L. V. Berkner and S. L. Seaton, Terr. Mag., **45,** 419 (1940).
[3] E. V. Appleton and W. R. Piggot, Nature, **165,** 130 (1950).
E. V. Appleton and W. R. Piggot, J. Atmosph. Terr. Phys., **2,** 236 (1952).
D. F. Martyn, Proc. 2nd Meeting, Mixed Comm. Ionosphere, 49 (1951),
Proc. Roy. Soc. A., **218,** 1 (1953).
H. Uyeda and Y. Arima, Rep. Ionosphere Res. Japan, **6,** 1 (1952).
T. Obayashi, Rep. Ionosphere Res. Japan, **6,** 79 (1952),
ibid., **8,** 135 (1954).
K. Miya and N. Wakai, Rep. Ionosphere Res. Japan, **6,** 137 (1952).
T. Nagata and T. Oguti, Rep Ionosphere Res. Japan, **7,** 21 (1953).
J. H. Meek, Geophys. Res., **57,** 117 (1952),
ibid., **58,** 445 (1953).
R. P. Waldo Lewis and D. H. MacIntosh, Atom. Terr. Phys., **3,** 186 (1953).
[4] Symposium on Ionospheric Storm, Rep. Ionosphere Res. Japan, **8,** (1954).
[5] K. Sinno, Rep. Ionosphere Res. Japan, **7,** 7 (1953).
[6] K. Sinno, ibid., **8,** 127 (1954).
[7] S. Chapman and J. Bartels, Geomagnetism, Oxford (1940).

Geomagnetic Distortion of the $F2$ Region on the Magnetic Equator

By Motokazu HIRONO and Hiroshi MAEDA
Geophysical Institute, Kyoto University

Abstract

The direct relation between the geomagnetic S_q variation and the vertical electron drift in the $F2$ region on the magnetic equator is examined.

It is shown that the electric field in the $F2$ region accompanied by S_q electric current produces the vertical drift which is sufficient to interpret the main features of the anomaly of the $F2$ region on the equator. It is to be noticed that the main term of the drift velocity is diurnal. The daily variations of the maximum electron density and its height in the $F2$ region are calculated under consideration of the vertical electron drift for the reasonable distribution of decay coefficient with altitude inferred by observed results. The calculated $F2$ daily variations have a striking resemblance with those observed near the magnetic equator. When the ion production takes its maximum value at about 200 km, there appears a lower secondary maximum of electron density which agrees well with the observed $F1$ layer.

The change of characteristics of daily variations of the $F2$ region with the sunspot-cycle is likely to be accounted for by a slight shift of the phase of the drift.

1. Introduction

Analyses of ionospheric data and theoretical researches by Martyn [1], Mitra [2] and Weiss [3] have established the existence of solar semi-diurnal components of tidal origin in the maximum electron concentration N_m of the $F2$ region and its height h_m, and further studies have been made by K. Maeda [4].

We tried to find a direct relation between the daily variation of the earth's magnetic field and the vertical electron drift in the $F2$ region on the magnetic equator.

McNish and Gautier [5] have attacked a similar problem, and an interesting relation between these data is shown. Their theoretical consideration is, however, confined to the vertical drift due to the electric field by the daily variation of the magnetic field, whereas the drift due to the electrostatic field is not taken into account. According to our results, the latter is so much greater than the former

that we disregarded the drift due to electromagnetic induction.

2. Observed Data of *F* Region near the Equator

The world-wide distribution of $N_m(F2)$ which is closely related with the earth's magnetic field was studied by Uyeda and others [6] and by Appleton [7]. Further studies have been made by Bailey [8], Uyeda [9] and Aono [10]. According to their results, for noon conditions, there is a belt of low values of $N_m(F2)$ circling the Earth and centred roughly on the magnetic equator, and the maximum value of $N_m(F2)$ is attained roughly at about the 20° north and south geomagnetic latitudes. The data analysed in detail came from eight widely distributed stations close to the magnetic equator and about the 20° geomagnetic latitudes (which will be referred to as Eq. and 20° stations respectively hereafter) for which the ionospheric characteristics at sp-maximum (sp=sunspot) and/or sp-minimum are well observed. All information was extracted from the "Ionospheric Data" of C.R.P.L., Boulder, except that of Palau. The stations used are shown in Table 1.

Table 1

Station	Geographic Lat.	Geographic Long.	Geomagnetic Lat.	Geomagnetic Long.	Geomagnetic Dip	Times Standard
Ibadan	7°.4N	4°.0E	10°.6N	74°.7E	−5°	0°
Tiruchy	10°.8N	78°.8E	1°.0N	148°.4E	4°	Local
Leyte	11°.0N	125°.0E	0°.2S	193°.8E	4°	135°E
Palau I.	7°.3N	134°.5E	3°.3S	156°.3W	2°	135°E
Christmas I.	1°.9N	157°.3W	2°.2N	88°.7W	6°	150°W
Huancayo	12°.0S	75°.3W	0°.6S	6°.2W	2°	75°W
Maui	20°.8N	156°.5W	20°.9N	88°.1W	40°	150°W
Trinidad	10°.6N	61°.2W	22°.0N	8°.3E	43°	60°W

The values of $N_m(F2)$ are calculated from f^0F2 and h_m from the value of $(M3000)F2$ which will be denoted by M, using a formula by Shimazaki [11], i.e.,

$$h_m = -176 + 1490/M \text{ (km)}.$$

Various daily variation curves are shown in Figs. 1, 2 and 3. To see the change of characteristics with the sp-cycle, lack of data is to be met with at times. Hence the data of the years as close as possible to sp-max. or sp-min. were used.

For Eq. stations the daily variations are averaged from one year and for 20° stations the N curves averaged from the Northern solstice, May, June, July and Aug., the E curves from the equinoctial months, Mar., Apr., Sept. and Oct., and the S curves from the Southern solstice, Nov., Dec., Jan. and Feb. For Huancayo, $h'F2$, $h'F1$ and $N_m(F1)$ are illustrated as well, and some data analysed by Martyn [1] are shown in addition.

It can be seen from the figures that the daily variations at Eq. stations bear a good resemblance, moreover they are very similar to those observed at summer conditions in the middle and high latitudes. The values of N_m and h_m at Eq. stations increase with the increasing sp-numbers. The values of $N_m(F2)$ and

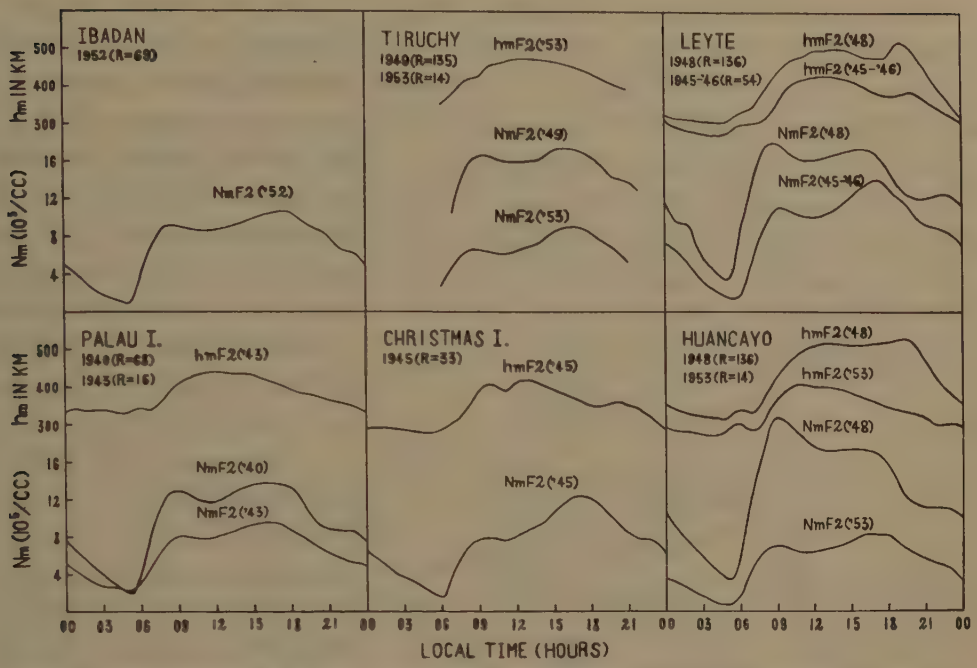

Fig. 1 Daily variations of $N_m(F2)$ and $h_m(F2)$ at stations close to the magnetic equator. The values of R denote the mean sunspot number for the year.

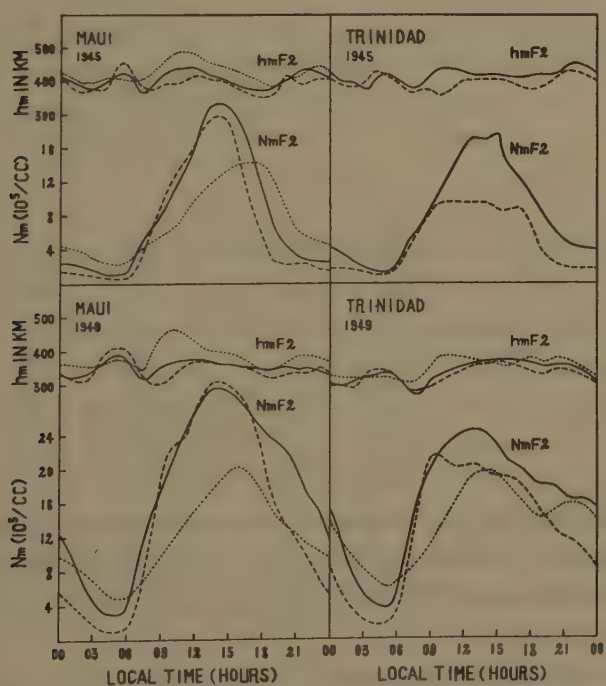

Fig. 2 Daily variations of $N_m(F2)$ and $h_m(F2)$ at stations of about 20° geomagnetic latitudes. Dotted lines refer to the northern solstice (N), dashed lines to the southern solstice (S), and full lines to the quinox (E).

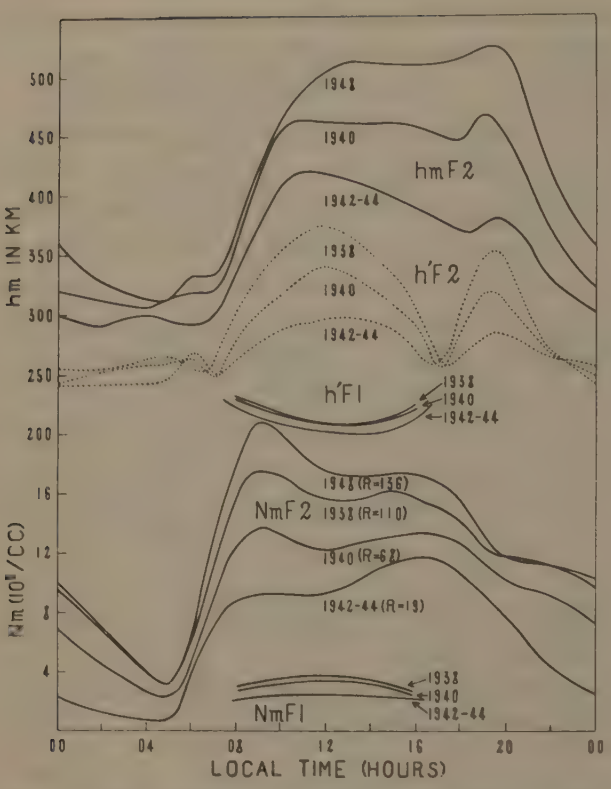

Fig. 3 Daily variations of $N_m(F2)$, $h_m(F2)$, $h'(F2)$, $N_m(F1)$ and $h'(F1)$ at Huancayo in years of different sun-spot numbers.

$N_m(F1)$ at noon of sp-max. at Huancayo are about 2.4 and 1.6 times of those at sp-min. The forenoon maximum of $N_m(F2)$ is smaller than the afternoon maximum of $N_m(F2)$ for the sp-minimum period. The former increases in relation to the latter with the increase of sp-number. At Huancayo, especially, the former is greater than the latter at sp-max.

The daily variations of $h_m(F2)$ at Huancayo and Maui were subjected to a harmonic analysis and the amplitudes P_n and phases t_n when maximum value was attained for nth term are shown in Table 2.

It can be seen from this table that at Huancayo the diurnal term is much greater than the semi-diurnal one, whereas at Maui the relation is reversed.

Table 2

Station	Year	Season	P_0 (km)	P_1 (km)	t_1 (hr.)	P_2 (km)	t_2 (hr.)	P_3 (km)	t_3 (hr.)
Huancayo	1942-44	mean	350	61.9	14.2	15.3	10.7	14.6	3.2
	1940	mean	394	87.8	14.9	13.7	9.7	16.0	3.2
	1948	mean	429	110.6	15.7	16.8	9.4	8.0	2.3
Maui	1945	N	327	28.0	12.0	30.1	0.6	4.6	4.6
	,,	E	306	9.2	9.6	21.7	10.9	16.8	5.3
	,,	S	294	14.2	6.3	8.6	10.7	25.6	5.6

3. Vertical Electron Drift of the *F* Region on the Magnetic Equator

(i) The motion of charged particles and the electrical conductivity of the ionosphere have been discussed by Hirono [12], [13], [14] (hereafter referred to as I, II and III respectively).

When the electric field attains such a value that the vertical electric current vanishes, the velocity of the vertical drift, which is the same for ions and electrons and measured positive upwards, is given on the magnetic equator, according to III, by

$$W=f(h)E_y/H, \qquad (1)$$

where H is the magnitude of the main magnetic field, and E_y is the eastward component of the electric field, and $f(h)\simeq p_i/(p_i+p_e)$ with $p_r=(1/m_r)\{\nu_r/(\nu_r^2+\omega_r^2)\}$, $(r=\text{i,e})$, where ν_i and ν_e are roughly the collision frequencies for ions and electrons; ω_i and ω_e are their frequencies of spiralling round the lines of magnetic force; m_i and m_e are their masses. For this expression, the particle concentration of negative ions is taken as effectively zero according to Bates and Massey [15].

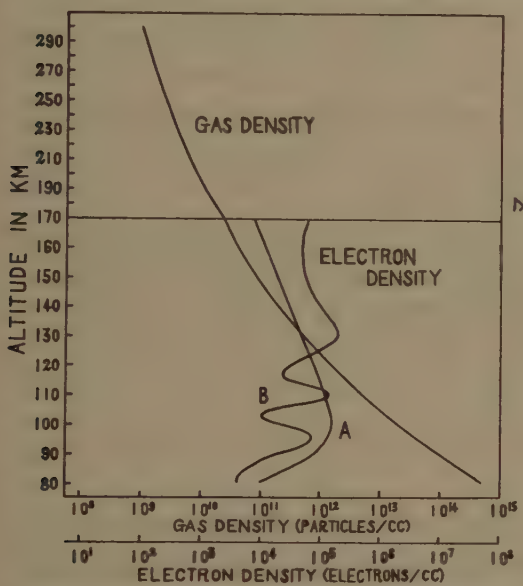

Fig. 4 Atmospheric model and distributions of electron density with altitude. Curve A denotes the Chapman layer, and curve B is inferred from rocket observations [21].

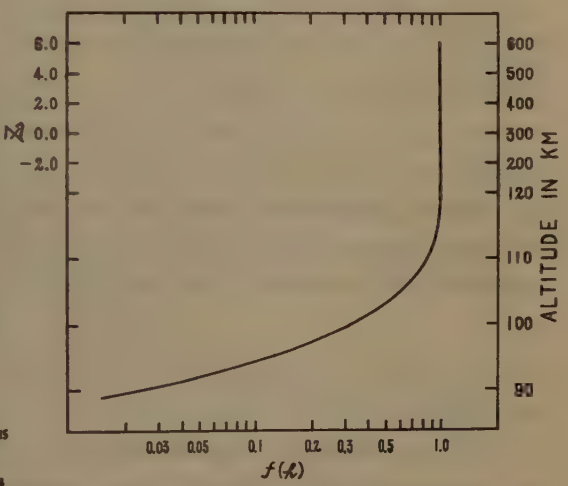

Fig. 5 Variation of $f(h)=W/(E_y/H)=p_i/(p_i+p_e)$ with altitude.

We adopt an atmospheric model inferred by rocket observation [16] as shown in Fig. 4 to which the following calculations refer. As illustrated in Fig. 5, $f(h)$ is nearly unity above the height of about 120km and decreases rapidly in the lower region. When the vertical current is not much greater than the horizontal one, Equation (1) holds approximately for the vertical electron drift in the F region.

(ii) According to the dynamo theory, the electromotive force of the S_q current on the magnetic equator is the electrostatic field. It is shown in II from the theory of potential that the eastward component E_y of this field is almost constant between the E and F regions.

The electrical conductivity of the ionosphere in the E-W direction is expressed, as shown in I, by

$$\sigma_3=\sigma_1(1+\sigma_2^2/\sigma_1^2),$$

where

$$\sigma_1=e^2\left(\frac{n_e}{m_e}\frac{\nu_e}{\nu_e^2+\omega_e^2}+\frac{n_i}{m_i}\frac{\nu_i}{\nu_i^2+\omega_i^2}\right),$$

$$\sigma_2=\frac{n_e\cdot e}{H}\left(\frac{\omega_e^2}{\nu_e^2+\omega_e^2}-\frac{\omega_i^2}{\nu_i^2+\omega_i^2}\right),$$

where n_e and n_i are particle concentrations of electrons and ions, and e denotes the absolute value of the charge of an electron. Let the eastward electric currents integrated with height in the E and F regions be I_1 and I_2 respectively, then we have approximately

$$I_1=K_1\cdot E_y, \qquad I_2=K_2\cdot E_y, \tag{2}$$

where

$$K_1=\int_E \sigma_3 dh, \qquad K_2=\int_F \sigma_3 dh.$$

According to II, III and H. Maeda [17], $K_1 \gg K_2$; therefore it follows that

$$I_1 \gg I_2.$$

Put $I_1+I_2=I$, and let the magnetic variation due to I at the lower edge of the E region be δH, then we have

$$\delta H=2\pi I \simeq 2\pi I_1. \tag{3}$$

Considering the fact that about 80 per cent of the daily magnetic variation ΔH on the ground is caused by I and that this magnetic field due to I increases upwards and the amount of the increase will be about 20 per cent at the lower edge of the E region [18], so that we have approximately

$$\Delta H \simeq \delta H \simeq 2\pi K_1\cdot E_y. \tag{4}$$

When the values of ΔH and K_1 are known, we can determine the value of E_y using this relation.

(iii) M. Hasegawa and H. Maeda [19] have estimated the daily variations of electrical conductivity of the S_q layers (mainly the E layer), and as a result of this analysis the daily variations of electric field and the zero level (C_0) of the S_q variations have also been estimated. Further, H. Maeda [20] has made his calculations on Huancayo's geomagnetic data for a period of 12 years, and the results for the mean states of sp-min. years, 1922, 23, 32 and 33, and sp-max. years, 1926-29, are as follows:

$$\Delta H=C_0+\sum C_n \sin(n\lambda+\varepsilon_n) \qquad (10^{-5}\text{e.m.u.}). \tag{5}$$

Years	Average sp-number (R)	C_0	C_1	ε_1	C_2	ε_2	C_3	ε_3
1922, 23 32, 33	8 (min)	15.1	32.5	280°.2	15.8	108°.4	5.8	306°.0
1926, 27 28, 29	71 (max)	24.3	52.4	274°.1	25.7	103°.9	10.9	302°.2

$$K_1=K_0\{1+\sum \gamma_n \cos(n\lambda+\delta_n)\} \qquad \text{(e.m.u.)}, \tag{6}$$

γ_1	δ_1	γ_2	δ_2
1.15	180°	0.42	0°

(almost independent of sp-number)

where λ is the local time is angular measure from midnight and ΔH is measured positive northwards. The daily variation of K_1/K_0 is shown in Fig. 6.

On the magnetic equator, Hall conductivities σ_{xy} and σ_{yx} vanish and Ohm's

law holds in its original form, so that the results estimated by the method of the above authors are theoretically adequate. The noon value of integrated conductivity of the E layer calculated as a simple Chapman layer of scale height=10km, maximum electron density at noon=1.5×10^5/c.c. (for sp-min.), height of maximum ion production =100km as shown by curve A in Fig. 4, is 3.4×10^{-7} e.m.u., so that from the relation (6) K_0 becomes 1.3×10^{-7}e.m.u. For the sp-max. period mentioned above we take $K_0=1.65\times10^{-7}$ e.m.u. corresponding to the maximum electron density of 1.9×10^5/c.c. for the E layer.

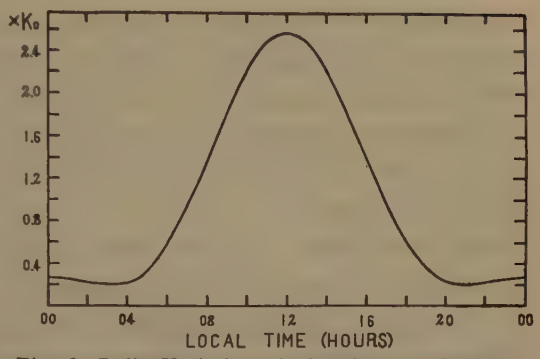

Fig. 6 Daily Variation of electrical conductivity in units K_0.

The electrostatic field E_y expressed in Fourier series does not include a constant term, since this is derived from the potential. Therefore we have the following expression of E_y and Table 3 in connection with relations (4), (5) and (6), using the value of K_0 estimated above:

$$E_y=y_1\sin(\lambda+\theta_1)+y_2\sin(2\lambda+\theta_2) \quad \text{(e.m.u.)}. \tag{7}$$

Table. 3

Years	y_1	θ_1	y_2	θ_2
sp-min.	3.34×10^2	280°	0.36×10^2	176°
sp-max.	4.19×10^2	265°	0.81×10^2	171°

If we take the value of H=0.27 gauss at the height of the F region over Huancayo, from (1) and (7) we have the following drift velocity:

$$W=f(h)\{W_1\sin(\lambda+\theta_1)+W_2\sin(2\lambda+\theta_2)\}, \tag{8}$$

where

$$\left.\begin{aligned} W_1&=1.24\times10^3\text{cm/sec.}\\ W_2&=0.13\times10^3\text{cm/sec.}\end{aligned}\right\}\ \text{for sp-min. period,}$$
$$\left.\begin{aligned} W_1&=1.55\times10^3\text{cm/sec.}\\ W_2&=0.30\times10^3\text{cm/sec.}\end{aligned}\right\}\ \text{for sp-max. period.} \tag{9}$$

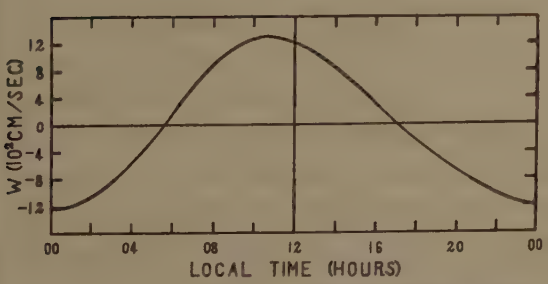

Fig. 7 Daily variation of vertical electron drift velocity W for sp-min. at a height of 300km referred to curve A in Fig. 4.

The daily variation of W for sp-min. at an altitude of 300km is shown in Fig. 7. The value of K_0 is influenced to some extent by the assumed electron density distribution with altitude. If the electron density above 100km is 1.5×10^5/c.c. and below that level the same as the above mentiond Chapman layer, K_0 is increased by about 10 per cent. This variation is very small.

On the other hand, when we adopt an electron density distribution with altitude inferred by rocket observation [21] as shown by curve B in Fig. 4, K_0 takes

one second of the above mentioned values, i.e., 6.5×10^{-8}e.m.u. for sp-min. and 8.3×10^{-8}e.m.u. for sp-max. If these values of K_0 are used, the electric field E_y and drift veloity W become twice as great as those represented by (8) and (9).

Effective conductivity σ_3 is obtained under the assumption that the electric and magnetic fields are completely uniform, therefore if they are not completely so, the effective conductivity in the E-W direction may be slightly less than σ_3. Then the decrease in K_0 will give slightly greater values for W in any case.

4. Solution of the Continuity Equations

Let unit of height $\mathfrak{H}$ be 50km and $z=(h-h_0)/\mathfrak{H}$, and let $z=0$ at an altitude of 300km. In the F region, the local scale height of the atmosphere $\mathfrak{H}(F)$ is taken to be the same as the height unit $\mathfrak{H}$, but in the E region the local scale height is taken to be a function of altitude which may be deduced from Fig. 4.

The equation of motion for an electron is $dh/dt=W$ which may be transformed to

$$\frac{dz}{d\lambda}=1.37\times10^{4}\frac{W}{\mathfrak{H}}. \tag{10}$$

The solution of this equation for a prescribed value of W may be written

$$z=z(z_0,\ \lambda), \tag{11}$$

with z_0 fixed by initial candi-tions at $\lambda=\lambda_0$.

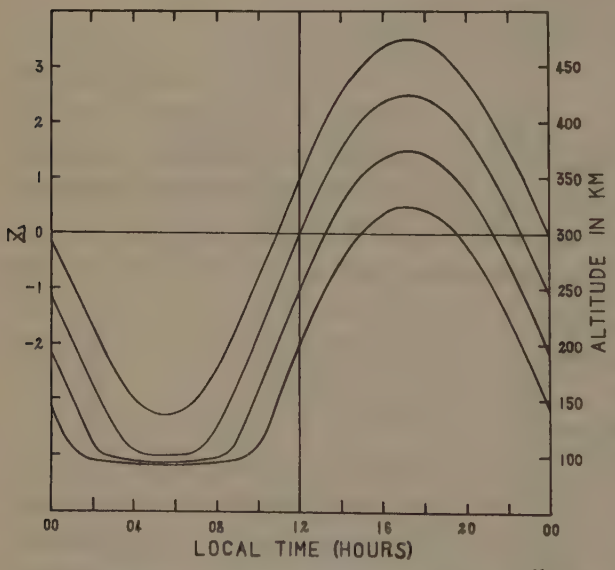

Fig. 8 Solutions of the subsidiary equation $\frac{dh}{dt}=W$ for some initial values of h.

In Fig. 8, several curves emerging from (11) derived from (8) and (9) for the sp-min. period are illustrated for some values of z. According to this figure, it was found that a part of the electrons in the $F2$ region descends at night and enters into the E region. In a later section, however, the results of calculation show that the electron densitiy in the cell, which descends below 300km, rapidly decreases because of a great recombination cofficient in the lower region, tending to be several times 10^4/c.c. and the electron density of the E region does not seem to be appreciably influenced, Thus, $h_m(F2)$ does not descend much below the 300km level.

(i) Theoretical discussion of the effect of the vertical electron drift upon an ionized region, necessitates a consideration of the equation of continuity

$$\frac{\partial N}{\partial t}=I-\alpha N^2-\frac{\partial}{\partial h}(N\cdot W), \tag{12}$$

where N stands for electron density per c.c., I for ion production per c.c. per sec., and α for the recombination coefficient. This equation is to be solved subject to the subsidiary condition (11) imposed by the drift.

In the F region W is estimated to be almost independent of altitude, so that we have

$$\frac{dN}{dt}=[I]_z-[\alpha]_z N^2, \tag{13}$$

where d/dt stands for a derivative "following the motion." In this equation I and α are to be evaluated at the height z which is obtained from (11) as a function of z_0 and t. It is shown by Bates and Massey [22] that $\alpha=8\times10^{-11}$c.c./sec. in the $F2$ region and $\alpha=4\times10^{-9}$c.c./sec. in the $F1$ region (independent of pressure) in the daytime. For the $F2$ region at night, Ratcliffe [23] obtained a recombination coefficient of the same order of magnitude as the above daytime value, in the absence of the vertical drift influence. Therefore, we take $\alpha=\alpha_0\xi(z)$, where $\xi(z)$ is taken to be unity for $z\geqq0$ and 50 for $z\leqq-1$ as illustrated in Fig. 9. For the electrons which have descended into the E region at night, a third term including the vertical gradient of W appears on the right hand side of (13). In the following calculation this term is neglected. According to the study by Weiss [3] on the variation of electron density at night, this neglection will be justified when we confine our attention to the daily variation of electron concentration in the F region. For the distribution of ion production, the following two types (a) and (b) are considered:

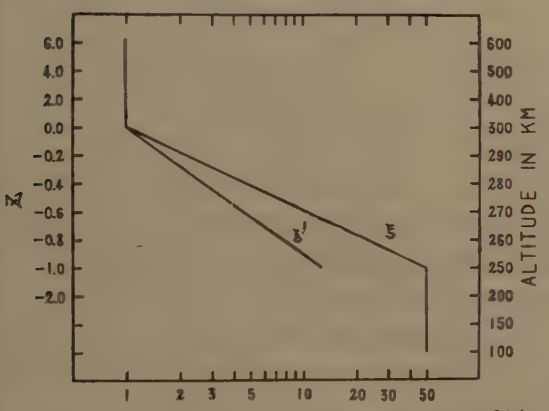

Fig. 9 Variation of $\xi(z)=\frac{\alpha(z)}{\alpha_0}$ and $\xi'(z)=\frac{\beta(z)}{\beta_0}$ with altitude.

(a) *The maximum of ion production at noon is located at* 300km.

According to S. Chapman [24]

$$I=I_0F(z,\ \chi),$$

where $F(z,\ \chi)=\exp\{1-z-\exp(-z)Ch(R+z,\ \chi)\}$, and $Ch(R+z,\ \chi)$ is a complicated function of R and the solar zenith angle χ, and $R=150$ is used here. After some transformation of (13) and by putting $N_0(a)=(I_0/\alpha_0)^{1/2}$ and $\nu=N/N_0$, we get

$$\sigma_a\frac{d\nu}{d\lambda}=[F]_z-[\xi]_z\nu^2, \tag{14}$$

where

$$1/\sigma_a=1.37\times10^4(I_0\alpha_0)^{1/2}.$$

(b) *The maximum of ion production at noon is located at* 200km.

Bradbury [25], Mohler [26] and Bates [27] suggested that the $F1$ and $F2$ layers are produced by the same atoms or molecules ionized by the same ultra-

violet, and the two layers are separated by a rapid change of the recombination coefficient with altitude. To examine the effect of the drift upon an ionized region under such conditions, we take $I=I_0F(z+2,\ \chi)$. Putting $N_0(b)=\{I_0F(2,\ 0)/\alpha_0\}^{1/2}$, $\nu=N/N_0$ and $F'=F(z+2,\ \chi)/F(2,\ 0)$ and after some transformation of (13), we get

$$\sigma_b\frac{d\nu}{d\lambda}=[F']_z-[\xi]_z\nu^2, \tag{15}$$

where $1/\sigma_b=1.37\times10^4\{I_0F(2,\ 0)\alpha_0\}^{1/2}$.

(ii) According to the theory of dissociative recombination by Bates and Massey [28], a recombination of electrons with ions might take place in the same form as that under the attachment law. Though this theory is not yet established quantitatively, we shall use the following equation in place of (13)

$$\frac{dN}{dt}=[I]_z-[\beta]_zN. \tag{16}$$

We take $\beta=\beta_0\xi'$, and the variation of ξ' with altiude for $z>-1$ is taken as shown in Fig. 9, and $\beta_0=8\times10^{-5}$/sec. is adopted from the relation $\beta_0=N_0\alpha_0$. Ion production is taken as type (b), i.e. $I_0=I_0F(z+2,\ \chi)$. Putting $F'=F(z+2,\ \chi)/F(2,\ 0)$, $N_0(c)=I_0\cdot F(2,\ 0)/\beta_0$ and $\nu=N/N_0$,we have

$$\sigma_c\frac{d\nu}{d\lambda}=[F']_z-[\xi']_z\nu, \tag{17}$$

where $1/\sigma_c=1.37\times10^4\beta_0$. For the altitudes $z\leqq-1$, (15) is used instead.

5. Distortion of the F Region by Drift subject to S_q Current

To evaluate the effect of S_q drift on the F region on the equator, we solved Equations (14), (15) and (17) following the motion subject to the subsidiary condition (11) using the method of Millington [29]. Numerical integration is made at an interval of 10° of local time λ, but between the height $-1<z<0$ the interval was taken to be 5°. Using these solutions, the maximum electron density ν_m in units of N_0 and its height $h_m(=z_m\cdot\mathfrak{H}+300\text{km})$ are illustrated in Fig. 10. The details of the cases calculated are summarized in Table 4.

Table 4

Case	Continuity Equ. used	Drift Velocity				Curve in Fig. 10 illustrating
		W_1(cm/sec)	θ_1	W_2(cm/sec)	θ_2	
1	(14) with $\sigma_a=1$	1.24×10^3	280° ($11^h.3\uparrow$)	0.13×10^3	176°	(a), Curve A
2	,,	2.48 ,,	,,	0.26 ,,	,,	,, B
3	(15) with $\sigma_b=1$	1.24 ,,	,,	0.13 ,,	,,	(b), Curve A
4	,,	2.48 ,,	,,	0.26 ,,	,,	,, B
5	(14) with $\sigma_a=1$	1.24 ,,	0° ($6^h.0\uparrow$)	0		(c), Curve A
6	,,	,, ,,	180° ($18^h.0\uparrow$)	0		,, B
7	(17) with $\sigma_c=1$	,, ,,	280°	0.13×10^3	176°	(d)
8	(14) with $\sigma_a=1/2$	,, ,,	,,	,, ,,	,,	(e)
9	(15) with $\sigma_b=1/1.5$	2.48 ,,	,,	0.26 ,,	,,	(f)
10	(15) with $\sigma_b=1/1.5$	3.10 ,,	265° ($12^h.3\uparrow$)	0		(g)
11	(15) with $\sigma_b=1$	2.48 ,,	250° ($13^h.3\uparrow$)	0		(h)
12	(15) with $\sigma_b=1$	2.48 ,,	220° ($15^h.3\uparrow$)	0		(i)

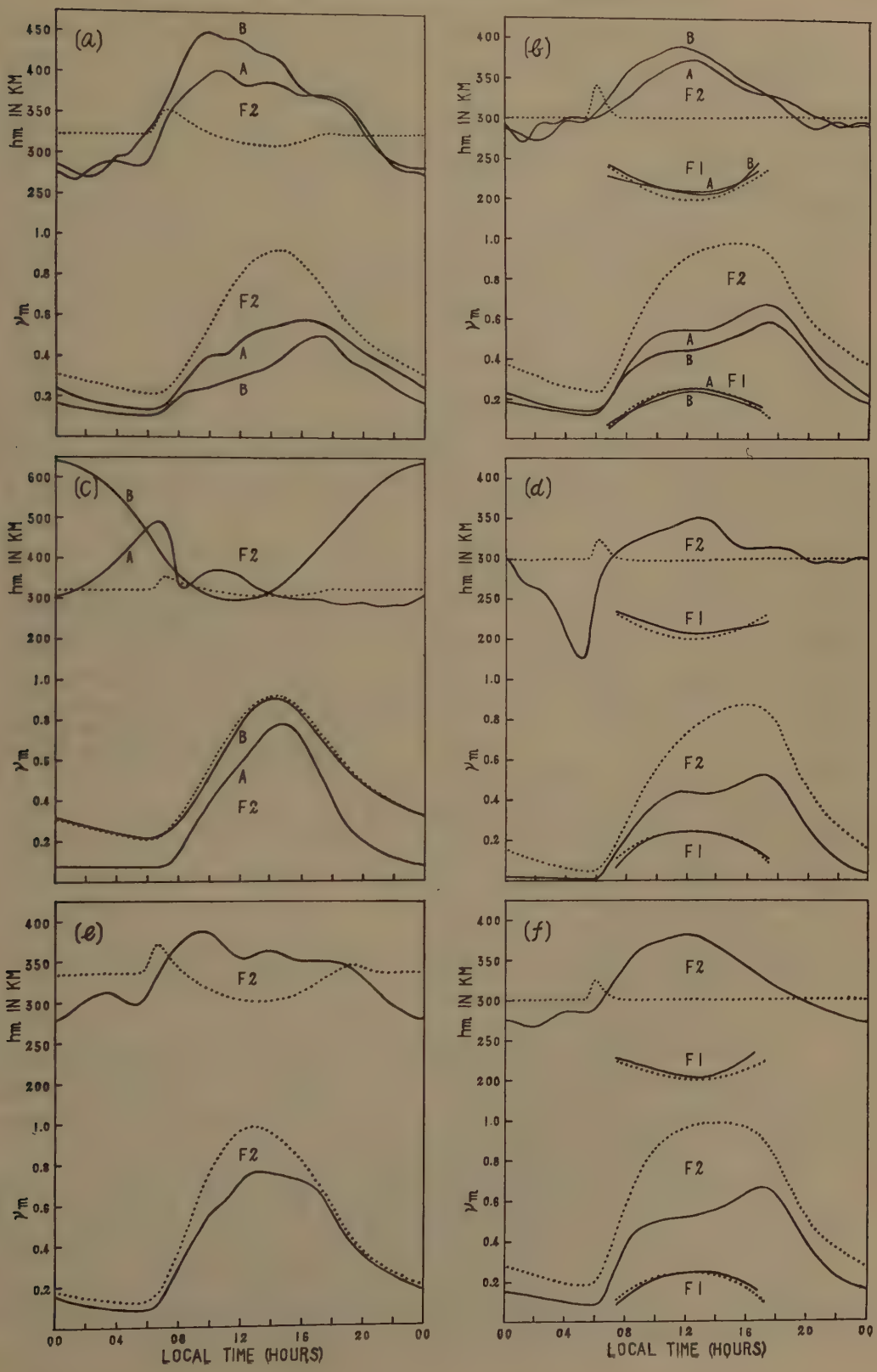
(a)
(b)
(c)
(d)
(e)
(f)
hm IN KM
γm
B
A
F2
F1
00 04 08 12 16 20 00
LOCAL TIME (HOURS)

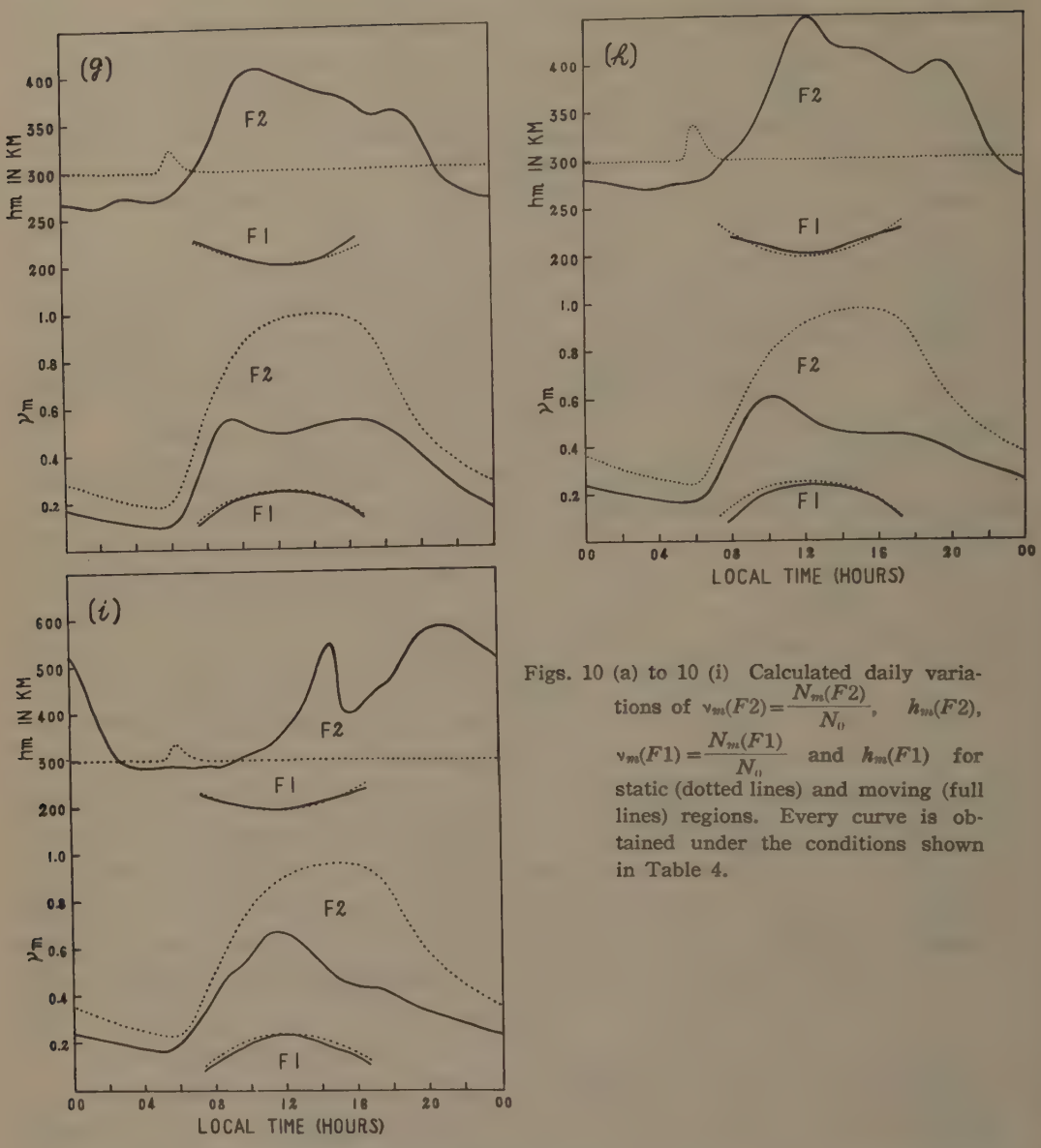

Figs. 10 (a) to 10 (i) Calculated daily variations of $\nu_m(F2)=\frac{N_m(F2)}{N_0}$, $h_m(F2)$, $\nu_m(F1)=\frac{N_m(F1)}{N_0}$ and $h_m(F1)$ for static (dotted lines) and moving (full lines) regions. Every curve is obtained under the conditions shown in Table 4.

(i) In the $F2$ region it is estimated that σ_a, σ_b and σ_c in (14), (15) and (17) are close to unity. Therefore Cases 1 to 4 in Table 4 are calculated. In any case the corresponding values ν_{0m} and h_{0m} for the static Chapman layer are shown in the same figure but by dotted lines.

The variations of ν_m and h_m of these four cases are very similar to those observed at Huancayo and other Eq. stations, at the period of minimum and moderate sp-numbers. In general ν_m is smaller than ν_{0m}, and at noon the decrease $\delta\nu_m$ from ν_{0m} is between 40 and 60 per cent, and the maximum of ν_m is attained in the afternoon. The daily variations of h_m are subjected to harmonic analysis, and the amplitudes P_n and phases t_n of the terms are shown in Table 5.

Comparing these values with those calculated from the observed data at Huancayo (1942–44) as shown in section 2, it is to be noticed that Cases 1 and 4 fit well with those observed. However, so far as ν_m is concerned, Cases 3 and 4 are in better agreement with those observed, moreover in the two cases there appears a lower secondary maximum of electron density which may be termed as $\nu_m(F1)$.

Table. 5

Case	P_0 (km)	P_1 (km)	t_1 (hr.)	P_2 (km)	t_2 (hr.)	P_3 (km)	t_3 (hr.)
1	338	62.5	13.3	7.9	9.1	13.4	1.8
2	347	82.4	12.4	15.9	10.2	8.3	2.3
3	321	36.1	12.6	9.3	0.2	6.4	2.7
4	326	51.3	12.0	10.7	11.1	2.1	7.6

The daily variations of $\nu_m(F1)$ and its height $h_m(F1)$ does not show appreciable departures from static Chapman norm because of a great recombination coefficient and ion production in the altitudes. At noon we have $\nu_m(F1)N_0(b)=2.5\times10^7$/c.c., if we take $N_0(b)=10^6$/c.c., and at the same time $h_m(F1)\simeq200$ km. Thus, the lower layer is very similar to the observed $F1$ region.

(ii) The question may arise, whether or not the drift W with other phases than those derived from (7) have similar affects upon the ionized region. To answer this question Cases 5 and 6 have been calculated. The variations of h_m in these cases do not resemble those observed near the magnetic equator. The variations of ν_m do not show appreciable departures from the static Chapman norm ν_{0m}, and especially in case 6 we see that $\nu_m\simeq\nu_{0m}$. If the value of W appropriately tekes less value in case 6, ν_m will be greater than ν_{0m} by about ten per cent, since in this case the motion of a cell is in phase throughout the day with the motion of the level of maximum ion production.

(iii) Case 7 was calculated to find the daily variation under the attachment law. In this case the variation of ν_m in the daytime resembles those observed, but at night ν_m is too small compared with those observed. Better results may be obtained for different values of β, but further discussion is not included in the present paper.

(iv) Cases 8 and 9 were calculated to evaluate the effect of the decrease of σ_a and σ_b. In Case 8, the effect of the drift upon the $F2$ region is a little decreased compared with Case 1. The calculated value of $N_m(F2)=\nu_m\cdot N_0(a)$ at noon for this case increases by a factor of 3 compared with that for Case 1, while $N_0(a)$ by a factor of 2.

In Case 9, the calculated $N_m(F2)$ and $N_m(F1)$ at noon increase by factors 1.8 and 1.5 respectively compared with those of Case 4, while $N_0(b)$ by a factor of 1.5.

Though at present we have no firm ground to assert that σ_a and σ_b are closer to unity at the period of sp-minimum, the above mentioned relative variations will throw some light on the variation of the $F2$ region due to the sp-numbers as mentioned in section 2.

(v) As shown in Table 3 the phase θ_1 of the diurnal term of E_y for the sp-max. period is 265° instead of 280° for sp-min. The range of errors for the

phases may be several degrees at present stage of calculation and much significance may not be attached to the difference of phases unitil further confirmed. Moreover the value of E_y in the E and F regions may not be strictly the same, and the difference may be 10 or 20 per cent. To find the change of characteristics of daily variations with the anticipated phase-shift of E_y and hence of W, Cases 10 and 11 (shown in Table 4) were calculated for the phases of W ($12^h.3\uparrow$) and ($13^h.3\uparrow$).

As before, in these cases two maxima of ν_m appear in the fore- and afternoon. The forenoon maximum is of an order of magnitude almost comparable with the afternoon maximum for Case 10 and the former is greater than the latter for Case 11. Moreover for Case 11 after sunset rapid increase of h_m appears for about one hour and is followed by the gradual decrease. These characteristics in the daily variations of ν_m and h_m are very similar to those observed at sp-max. at Eq. stations.

The course of the electron density contours *vs.* altitude throughout the 24 hours period for Cases 4 and 10 are illustrated in Fig. 11.

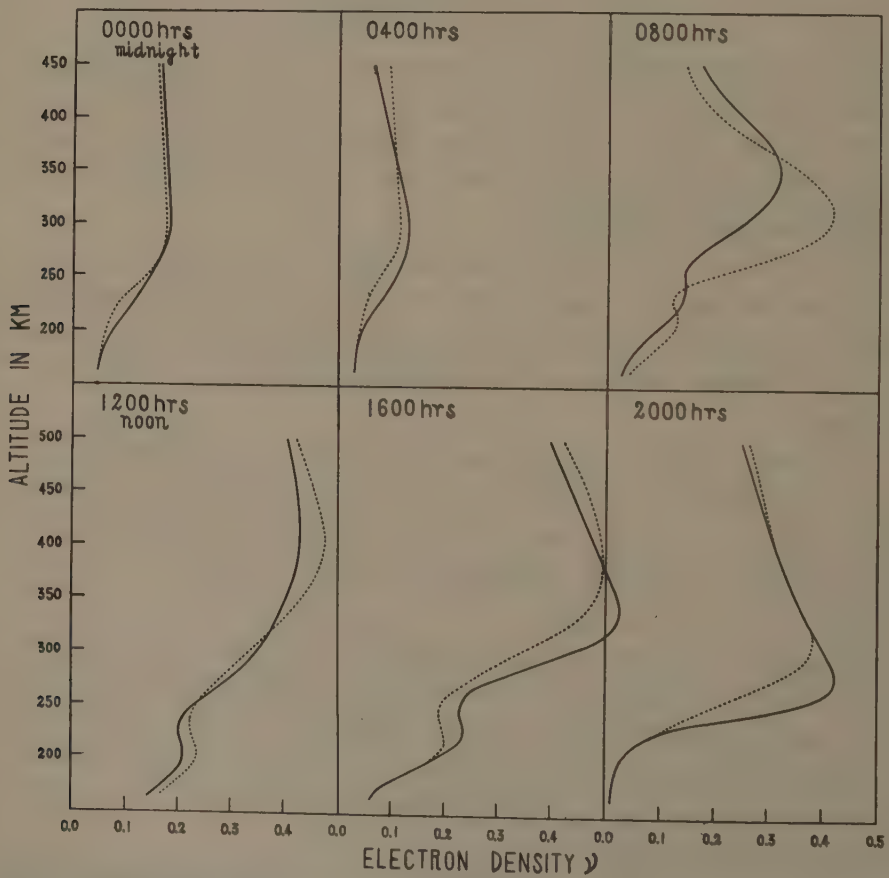

Fig. 11 Electron density contours *versus* altitude for Cases 4 (full lines) and 10 (dotted lines) shown in Table 4.

(iv) To examine the conditions leading to the sunset increase of h_m which is a remarkable characteristic of equatorial h_m variation, Case 12 was calculated under the assumption of further phase lag of W. In this case the sunset increase of h_m is further magnified, but the time of maximum h_m lags by about 2 hours beyond that observed, and in the day time the variation of h_m does not resemble those observed at Eq. stations. One maximum of ν_m appears at about 11.5 hr.

(vii) For Cases 1 to 4 the phase of W is ($11^h.3\uparrow$) and the daily variation of the calculated $F2$ region is very similar to those observed under summer conditions in middle latitudes, and for Case 6 the phase of W is ($18^h.0\uparrow$) and the daily variations are very similar to those observed under winter conditions in middle latitudes, if semi-diurnal variations are not taken into consideration. These characteristics will hold for the (b) type of ion production distribution as well. The seasonal variation of the $F2$ region in middle and high latitudes might thus be produced, if the diurnal drift velocity changes with season and the ion production takes appropriate forms.

6. Discussion of the Results

(i) When Weiss [3] discussed the effect of the semi-diurnal drift upon the $F2$ region, the amplitude of the drift was taken to be $0.5\mathfrak{H}(F2)$/hr., and the maximum departure of ν_m from the Chapman norm was 0.14. Here we used the drift velocity, which is almost an diurnal term and the amplitude of which is $0.893\mathfrak{H}(F2)$ $-1.785\mathfrak{H}(F2)$/hr. Hence departures from the static Chapman norm are much greater than those obtained by Weiss.

(ii) To discuss the variation of h_m, Martyn [1] neglects the first and second terms of the right hand side of (12) and uses the equation $\partial N/\partial t=-\partial(N\cdot W)/\partial h$. Therefore if use is made of $W=W_n\sin(n\lambda+\theta_n)$ which is independent of altitude, the following equation is obtained:

$$\Delta h_m=(W_n/n\omega)\sin(n\lambda+\theta_n-\pi/2), \tag{18}$$

wnere $\omega=7.3\times10^{-5}$.

If, as in the present treatment, $W_1=1.24\times10^3$cm/sec. is taken, the ampltude of Δh_m equals $W_1/\omega\simeq170$km. On the other hand, according to calculated results, the amplitude of Δh_m is about 60km, and is much less than that calculated by (18). Thus, if one uses (18) to obtain the drift velocity from the observed data, fairly great error will be introduced.

(iii) According to observed results near the equator, the increase of electron density at dawn begins at about 5 hr., but the calculated increase lags about one hour or more in any case, than those observed. This is due to the fact that ion production before ground sunrise is very small, even for type (b) in section 4. The early increase may be due to photo detachment by visible solar radiation from the negative ions formed gradually at night by molecular oxygen which is suggesed by Nicolet and Mange [30] to have a fairly great concentration in the $F2$ region,

(iv) The distribution with altitude of recombination coefficient used in section 4 may be somewhat different from the real one, so that the present calculation shows only a rough order of magnitude.

(v) The electrical conductivity of the E region and its variation mentioned in section 3 seem to be plausible to fit the estimation by radio observation [31] but observations of the electron density of the E region at night are still too meagre to confirm this situation.

For the electric field E_y obtained by H. Maeda [20], the diurnal term is about seven times that of the semi-diurnal one. This result is quite different from Martyn's conclusion [1] that the main term of the electric field for S_q is semi-diurnal. The variations of ν_m and h_m obtained here based on (8) agree with observed results. On the other hand the results calculated by Weiss [3] based on the semi-diurnal drift do not resemble those observed on the equator. The effect of the daily variation of the temperature upon the $F2$ region has been examined by Weiss [32] and Shimazaki [33] and it is seen that the effect is very small compared with those obtained here.

7. Distribution of the $F2$ Region near the Magnetic Equator

In the following, we shall evaluate the effect of the drift in the neighbourhood of the magnetic euator. The main magnetic field has been taken as that of a dipole with its axis coincident with that of the earth's rotation. The vertical drift velocity W in the F region can be written, using Equation (2) in III, as shown by Martyn [1],

$$\begin{aligned} W &= (E_y/H)\cos\phi = \{(Y-uH_z)/H\}\cos\phi \\ &= (Y/H)\cos\phi + (1/2)\cdot u\cdot\sin 2\phi, \end{aligned} \tag{19}$$

where Y is the eastward component of the electrostatic field, and u is the southward component of horizontal air velocity and H_z is vertical component of H measured positive upwards. Below an altitude of about 140km the value W/E_y decreases rapidly downwards except close to the magnetic equator.

From the theory of potential, the diurnal electrostatic field expressed by $y_1\sin(\lambda+\theta_1)$ in (7) may be fairly uniform between $\pm 20^\circ$ of latitude. However, Ampere force will accelerate the southward component of the air motion in the $F2$ region in such a way that the value of the diurnal component of E_y and hence of W at about 20° is much smaller than that at the equator and the phase of the former proceeds that of the latter by an amount not far from 90° in a similar way as shown in III (§ 10).

Referring to Case 5 of Fig. 12, a decrease of ν_m in the $F2$ region from ν_{0m} at noon by the drift at 20° will be very small, and moreover the ion production in these latitudes is roughly the same as at the equator. According to Weiss, the effect of the semi-diurnal drift upon ν_m is very small. It would therefore be possible that $N_m(F2)$ at 20° would be greater than that at the equator.

Complete treatment of this problem is, however, very difficult until the dis-

tribution of electric field and air motion in the $F2$ region due to various causes is known for the whole earth.

8. Concluding Remarks

From the foregoing analysis the following conclusion may be drawn:

The eastward component of the electric field producing the S_q current on the magnetic equator produces the vertical drift of the $F2$ region at the same time, the main term of the drift velocity is diurnal. The calculated daily variations of the $F2$ region, under consideration of this drift, have a striking resemblance with those observed near the magnetic equator. Moreover when the ion production take its maximum value at about 200km, there appears a lower secondary maximum of electron density which agrees well with the observed $F1$ layer in its density and altitude characteristics.

The change of characteristics of the daily variation of the $F2$ region with an sp-cycle seems to be accounted for by a variation in ion production and by a slight shift in the phase of the diurnal drift.

The daily $F2$ variations of the equatorial type have a resemblance with those under summer conditions in middle and high latitudes and when the drift velocity has such a phase ($18^h.0\uparrow$) as used in Case 6, daily variations are very similar to the observed diurnal variation in winter conditions in the latitudes. Thus the seasonal variation of the $F2$ region in the middle and high latitudes may be greatly influenced by the seasonal variation of the diurnal drift.

Acknowledgements

The authors wish to express their heartfelt thanks to Professor M. Hasegawa of Kyoto University for his continued interest and advice and to Professor K. Maeda of Kyoto Uiversity and Professor T. Nagata of Tokyo University for their valuable discussions.

References

[1] D.F Martyn, Proc. Roy. Soc. A, **189**, 241 (1947); *ibid.*, **190**, 273 (1947); *ibid.*, **194**, 429 and 445 (1948).

[2] A.P. Mitra, J. Atmosph. Terr. Phys., **1**, 286 (1951).

[3] A.A. Weiss, J. Atmosph. Terr. Phys., **3**, 20 (1953).

[4] K. Maeda, J. Geomagn. Geoelectr., **4**, 20 and 83 (1952); Rep. Ionosph. Res. Japan, **7**, 81 (1953).

[5] A.G. McNish and T.N. Gautier, J. Geophys. Res., **54**, 181 (1949).

[6] K. Maeda, H. Uyeda, and H. Shinkawa, Rep. Res. Phys. Inst. Rad. Waves, Nos. 1, 2 and 3 (1942).

[7] E.V. Appleton, Nature, **157**, 691 (1946); J. Atmosph. Terr. Phys., **1**, 106 (1950).

[8] D.K. Bailey, Terr. Magn., **53**, 35 (1948).

[9] H. Uyeda, Rep. Res. Phys. Inst. Rad. Waves, No. 8 (1948).

[10] Y. Aono, Rep. Ionosph. Res. Japan, **6**, 69 (1952); *ibid.*, **7**, 30 (1953).
[11] T. Shimazaki, J. Radio. Res. Lab. Tokyo, **2**, (to be published).
[12] M. Hirono, J. Geomagn. Geoeletr., **2**, 1 (1950); *ibid.*, **2**, 113 (1950).
[13] M. Hirono, J. Geomagn. Geoelectr., **4**, 7 (1952).
[14] M. Hirono, J. Geomagn. Geoelectr., **5**, 22 (1953).
[15] D.R. Bates and H.S.W. Massey, J. Atmosph. Terr. Phys., **2**, 1 (1951).
[16] R.J. Havens, R.T. Koll, and H.E. LaGow, J. Geophys. Res., **57**, 59 (1952).
[17] H. Maeda, J. Geomagn. Geoelectr., **5**, 94 (1953).
[18] S.F. Singer, E. Maple, and W.A. Bowen, J. Geophys. Res., **56**, 265 (1951).
[19] M. Hasegawa and H. Maeda, Rep. Ionosph. Res. Japan, **5**, 167 (1951).
H. Maeda, Rep. Ionosph. Res. Japan, **6**, 155 (1952).
[20] H. Maeda, Rep. Ionosph. Res. Japan, **9**, (to be published).
[21] W.W. Berning, Rocket Exploration of the Upper Atmosphere, London, Pergamon Press Ltd., p. 261 (1954).
J.R. Lien, R J. Marcou, J.C. Ulwick, J. Aarons, and D.R. McMorrow, *ibid.*, p. 223 (1954).
[22] D.R. Bates and H.S.W. Massey, Proc. Roy. Soc. A, **187**, 261 (1946).
[23] J.A. Ratcliffe, Proc. Mixed Commission on the Ionosphere, third meeting, p. 30 (1953).
[24] S. Chapman, Proc. Phys. Soc., **43**, 26 and 483 (1931); *ibid.*, **66**, 710 (1953).
[25] N.E. Bradbury, Terr. Magn., **43**, 55 (1938).
[26] F.L. Mohler, Bur. Stand. Jour. Res., **25**, 507 (1940).
[27] D.R. Bates, Proc. Roy. Soc. A, **196**, 562 (1949).
[28] D.R. Bates and H.S.W. Massey, Proc. Roy. Soc. A, **192**, 1 (1947).
[29] G. Millingtion, Proc. Phys. Soc., **44**, 580 (1932).
[30] M. Nicolet and P. Mange, J. Geophys. Res., **59**, 15 (1954).
[31] J.M. Watts and J.N. Brown, J. Geophys. Res., **59**, 71 (1954).
[32] A.A. Weiss, Austr. J. Phys., **6**, 291 (1953).
[33] T. Shimazaki, J. Geomagn. Geoelectr., **6**, 68 (1954).

Reverse and Normal Magnetism of the Basaltic Lavas at Kawajiri-misaki, Japan

By Eizo ASAMI

Physical Institute, Faculty of Arts and Science, Yamaguchi University

(Read Oct. 31, 1953 and Nov. 3, 1954)

Abstract

The early Pleistocene basaltic lavas at Kawajiri-misaki (Cape Kawajiri) have in general reverse natural remanent magnetism (N.R.M.), while at a part of the place both specimens of reverse and normal N.R.M. are found with their positions as intermixed, despite that they have been taken from the same rock block, and with their intensities ranging from 10^{-4} to 10^{-2}c.g.s.e.m.u./g. This fact seems to suggest that there is much room for the discussion regarding the idea that the reverse N.R.M. of the lavas would have been caused by a reverse geomagnetic field assumed to have occurred at the age of the ejection of the lavas.

The reverse N.R.M. of the basaltic lavas at Kawajiri-misaki situated at the Japan Sea coast of Yamaguchi Prefecture in west Japan was first reported by the present author [1] in 1954. From the thermo-magnetic studies of reversely magnetized igneous rocks in Japan (including the Kawajiri-misaki basalts), T. Nagata and others [2] have recently inferred that the direction of geomagnetic field at the time of formation of some of these rocks was reverse to that of the present.

However, the present author has left room for doubt of the above inference and for the purpose of further clarification of the fact he has again made a trip to Kawajiri-misaki and sampled more numerous basalt specimens from there. And the N.R.M. of these specimens have been measured in his laboratory. The results will be shown below.

The age of eruption of the basaltic lavas of Kawajiri-misaki is generally considered to be the early Pleistocene and they are considered also generally to have undergone no conspicuous dynamical disturbances since their eruption. In Fig. 1, the marks of cross (×) represent the sampling spots where crop out solid blocks of lava flow and the numerals nearby represent the specimen numbers. The specimens were sampled from various spots as much as possible. However, the inner part of the cape is covered with ordinary soils and the specimens could not be sampled from there. Thus, the author has measured the directions and intensities of magnetization of these 193 specimens collected solely from the areas

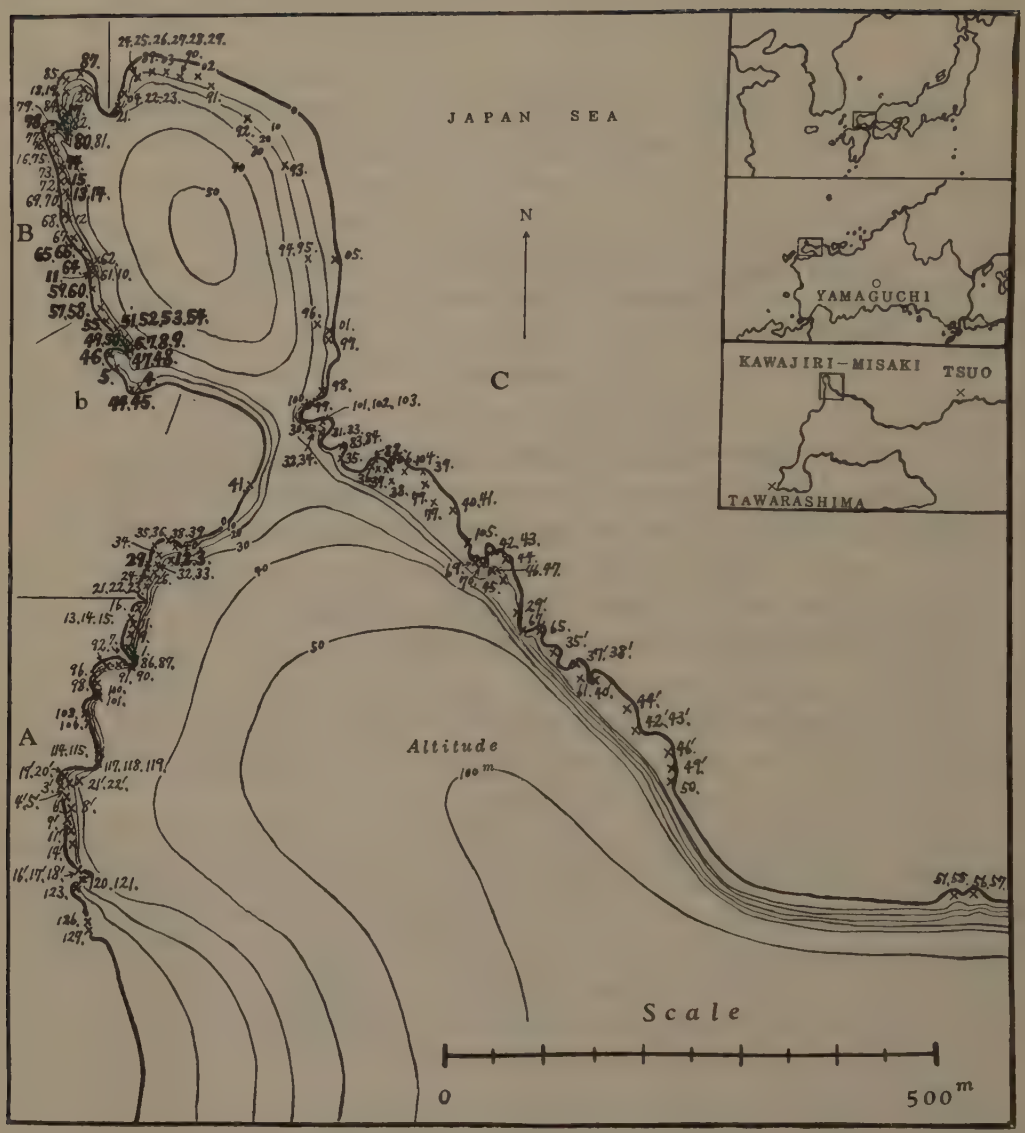

Fig. 1 Sampling spots at Kawajiri-misaki.
Thick numerals represent the specimen numbers of normal N.R.M. and thinn those of reverse N.R.M.

fringing the coast by means of an astatic magnetometer and obtained the following results.

In the first place, it is worth noting that the directions of the N.R.M of the specimens show a remarkable distribution; that is, in the belt C (Fig. 1) occupying the eastern coast and also in the belt A occupying the southern half part of the western coast the magnetizations are all reverse, while in the belt B occupying the northern half part of the western coast the normal and the reverse magnetizations are intermixed in positions and in the partial belt b occupying the middle part of the belt B the magnetizations are all normal.

Fig. 2 Directions of N.R.M. of the specimens in the belts A and C.

In Fig. 2 are shown the Schmidt's projections of the reverse magnetizations in the belts C and A, and in Fig. 3 those of the normal and the reverse magnetizations in the belt B with the partial belt b inclusive. In the both figures the vector of the present geomagnetic field whose dip is $+49°$ downward is represented by a thick cross (×).

The intensities of magnetization of the specimens are shown in Figs. 4, 5 and 6 by the lengths of the thick horizontal lines which are arranged on the ordinate in order of the positions of the spots the specimens have been taken from, the numerals nearby representing the specimen numbers.

The arithmetical average values of the directions and intensities of the N.R.M. and their ranges are shown in Table I. For the sake of reference, the similar quantities of the specimens from two places, one Tsuo (Fig. 1) 6km. to the east and the other Tawarashima 5km. to the south, of Kawajiri-misaki, are shown in Table II.

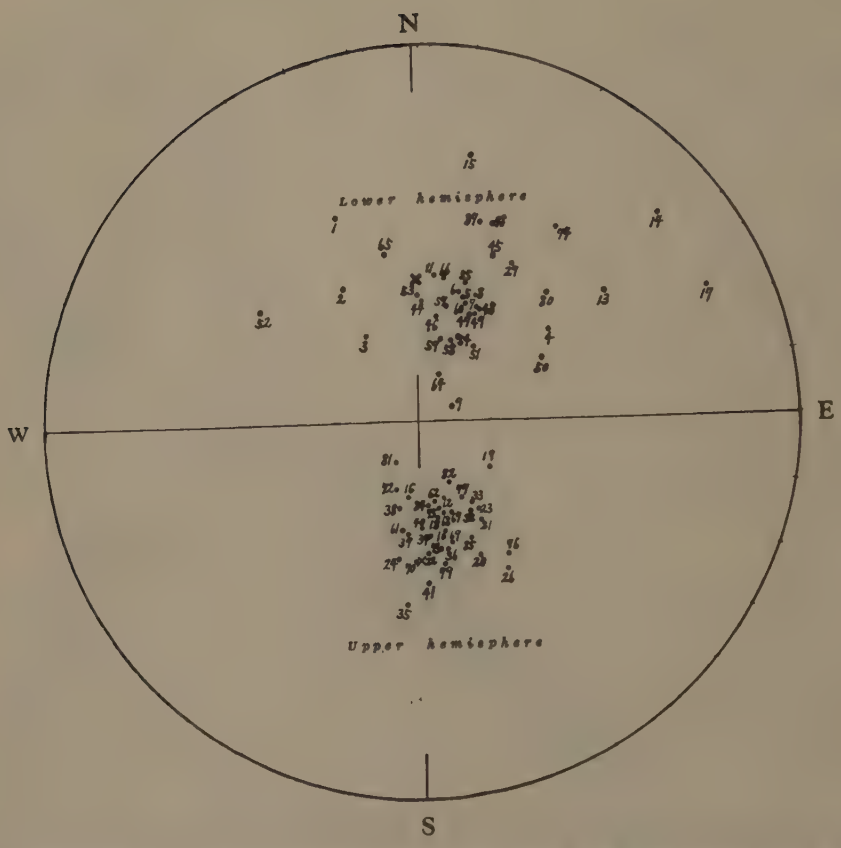

Fig. 3 Directions of N.R.M. of the specimens in the belt B with the partial belt b inclusive.

Table I N.R.M. of the Kawajiri-misaki basalts.

Locality	Normal or Reverse	Total number of the specimens	Declination		Dip		Intensity (10^{-3}c.g.s.e.m.u./g.)	
			Average value	Range	Average value	Range	Average value	Range
Belt B	Normal	38	N 21° E	N 54° W ~N 67° E	+46°	+ 9°~+80°	5.5	0.2~28.1
,,	Reverse	36	N169° E	N124° E ~N149 W	−57°	−38°~−75°	1.1	0.3~ 6.7
Belt A	Reverse	44	N160° E	N126° E ~N137 W	−47°	−23°~−71°	1.0	0.2~ 5.0
Belt C	Reverse	75	N168° E	N120° E ~N144 W	−55°	−32°~−74°	1.2	0.2~ 9.1
Total region	Reverse	155	N166° E	N120° E ~N137 W	−53°	−23°~−75°	1.1	0.2~ 9.1

Table II N.R.M. of the other basalts.

Tsuo	Normal	6	N22° E	N 8° E ~N 36° E	+35	+28 ~+52	1.3	0.5~2.1
Tawara-shima	Normal	5	N 1° E	N10 W ~N 14 E	+55°	+49°~+58°	1.4	0.6~2.0

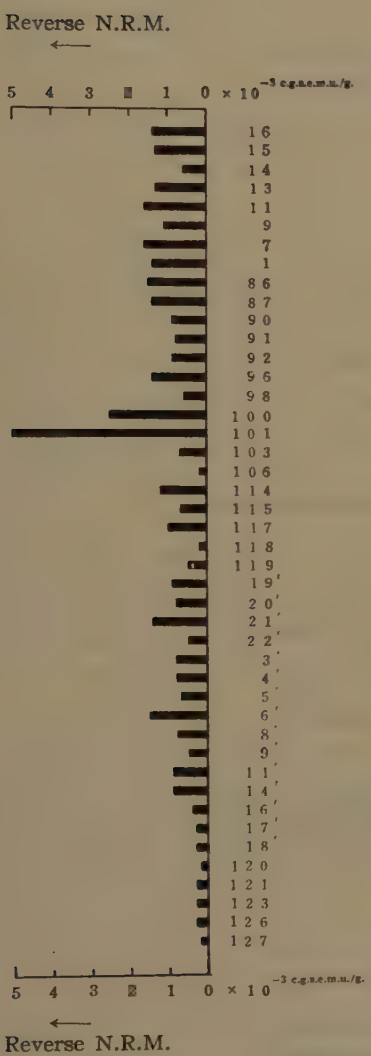

Fig. 4 Intensities of N.R.M. of the specimens in the belt A.

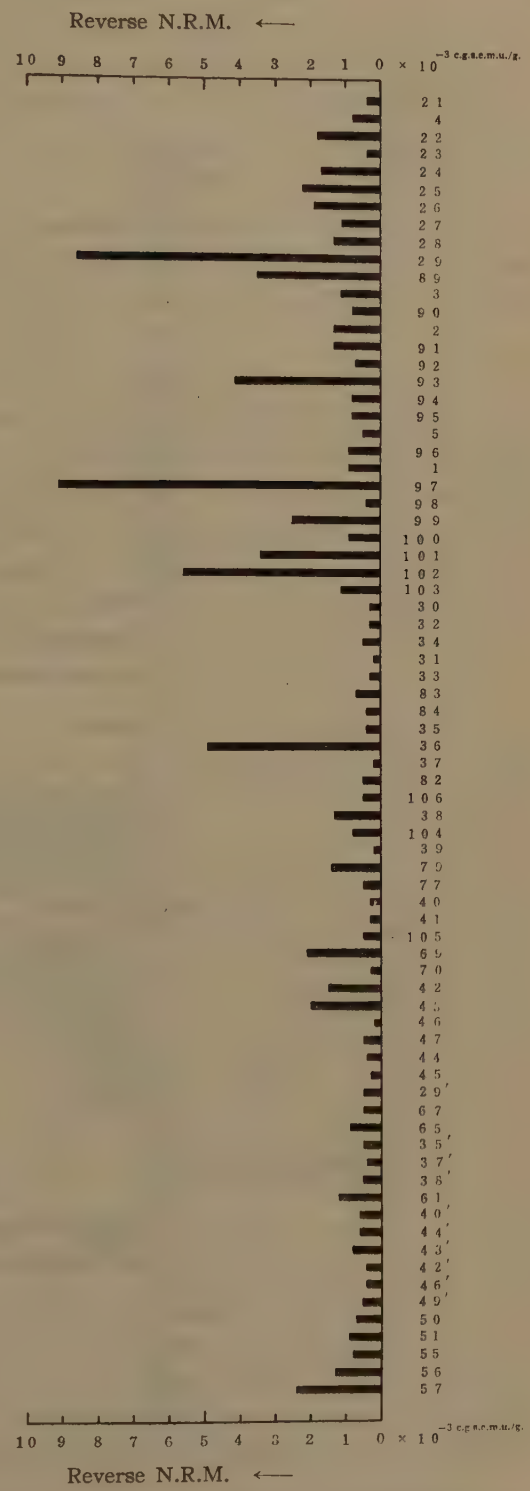

Fig. 5 Intensities of N.R.M. of the specimens in the belt C.

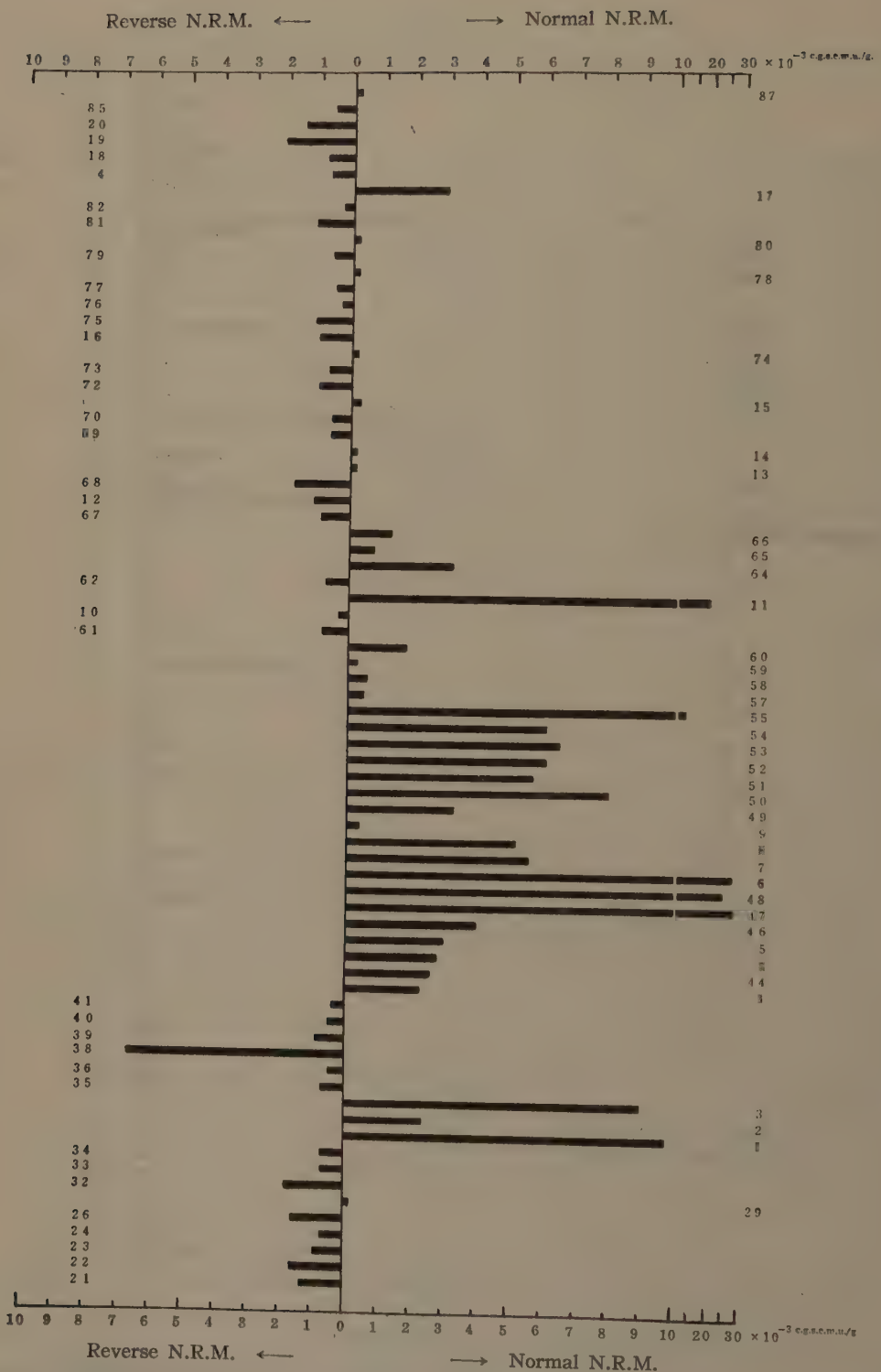

Fig. 6 Intensities of N.R.M. of the specimens in the belt B with the partial belt b inclusive.

Thus, the characteristics of the directions and intensities of the N.R.M. of the basaltic lavas at Kawajiri-misaki have been definitely clarified. Above all, the author has now recognized the decisive fact that the lavas at Kawajiri-misaki have in general reverse N.R.M., but at a part of the place both specimens of reverse and normal N.R.M. are found with their positions as intermixed, despite that they have been taken from the same rock block where any geological disturbances can hardly be noticed; for example, two specimens of normal No. 80 and reverse No. 81 have been taken from the spot considered to be the entirely same rock block in the northern part of the belt B (the distance separating the positions of these two specimens is only a few meters).

Moreover, as shown in Figs. 4, 5 and 6 and Tables I and II, the intensity of magnetization of these basalt specimens at Kawajiri-misaki is not uniform, while at all the other places [3] of Yamaguchi Prefecture, such as Tsuo, Tawarashima, it is fairly uniform and the N.R.M. is wholly normal. Roughly speaking, the average value of the intensities of magnetization of the specimens from Kawajiri-misaki is 10^{-2}c.g.s.e.m.u./g. for the normally magnetized basalts of the partial belt b, 10^{-3} for the reversely magnetized basalts of the total region and 10^{-4} for the normally magnetized basalts at the spots sandwiched between the spots of the reversely magnetized basalts of the belt B.

On the other hand, from the results of the thermo-magnetic study of our Kawajiri-misaki basalts, it has already been reported [2] that of both the reverse and normal specimens the N.R.M. is mainly due to the thermo-remanent magnetism and not to the local anomalous magnetization owing, for example, to thunderbolts.

It will be worth while to note that these facts may have a significant meaning for the study of palaeomagnetism. Generally speaking, if the igneous rocks have kept their N.R.M. stable since they acquired it as the thermo-remanent magnetism under the effect of the geomagnetic field in the remote epoch, it might be inferred that the direction of the N.R.M. represent that of the geomagnetic field at the time of formation of the rocks. It is generally believed that the thermo-remanent magnetism of stable ferromagnetic minerals only is able to remain stable during a long time. The above-mentioned facts seem to suggest that there is much room for the discussion regarding the inference [2] that the reverse N.R.M. of the lavas at Kawajiri-misaki would have been caused by a reverse geomagnetic field assumed to have occurred at the age of the ejection of the lavas. Because, should this inference be taken for granted, how could we explain the fact that at a part of the place the normal and the reverse magnetizations are intermixed in positions in the same rock block? If the normal or reverse of the directions of N.R.M. of rocks depend on that of the geomagnetic field, all specimens from the same rock block must show without exception only one side of either normal or reverse N.R.M..

However, it would be a little questionable whether the position intermixing

of the reverse and the normal magnetizations has taken place in the really same rock block or not. A key may, therefore, be afforded by a close geological field observation for confirming whether the normally magnetized rocks are dyke rocks penetrating the body of the reversely magnetized rocks or not. A more proper key would be the exact age determinations of both the reversely and the normally magnetized rocks.

On the other hand, another interpretation seems to be given, on the assumption that the above-mentioned fact has taken place in the really same rock block, by the idea most recently proposed by N. Kawai and others [4] that the magnetism of rocks cannot always be kept stable and the self-reversal of magnetization of rocks is possible to occur by a solid-phase transformation in ferromagnetic minerals responsible for the remanent magnetism of the rocks through a long period in geological time scale. The author has obtained the dependency of the intensity of saturation magnetization upon temperature for the several specimens from Kawajiri-misaki by means of a magnetic balance. From the result, it seems to be not particularly difficult to suppose that the facts found at Kawajiri-misaki may be in connection with this idea to some extent.

In concluding, the author wishes to express his sincere thanks to Dr. M. Matuyama, M.J.A., President of Yamaguchi University, for his kind direction throughout this research. His cordial acknowledgement is also due to Prof. N. Kumagai and Prof. M. Hasegawa of Kyoto University and Prof. T. Nagata of Tokyo University for their suggestive guidances and encouragements. He is also indebted to Mr. H. Domen for his assistance in this work.

References

[1] E. Asami, Proc. Jap. Acad., **30**, 102 (1954).

[2] T. Nagata, S. Akimoto, S. Uyeda, K. Momose and E. Asami, Tech. Comm. Palaeomagnetism, Xth Assembly, ATME, IUGG, Rome, 29 (1954).

[3] E. Asami and H. Domen, Jour. Yamaguchi Univ., **4**, 19 (1953), **5**, 29 (1954) (in Japanese).

[4] N. Kawai, S. Kume and S. Sasajima, Proc. Jap. Acad., **30**, 588, 864 (1954).

LETTERS TO THE EDITOR

On the Solar Lyman Beta Radiation and the Ionosphere

It has been known that there exists an atomospheric window at the wavelength of the Lyman beta line of hydrogen in the ionosphere [1]. R. v. d. Woolley suggested that the solar Lyman beta radiation emitted from the chromosphere would be an effective radiation which gives rise to the radio fade-out [2].

The Lyman beta line of hydrogen is, however, coincident with the radiation caused by transition between the ground 2^3P level and the excited 3^3D level of atomic oxygen in wavelength. [($L_\beta\lambda$ 1025Å, OI 2^3P-3^3D λ 1026Å) As atomic oxygen is one of the main constituents of the ionosphere in the E and F regions, the incident solar Lyman beta line will be absorbed by atomic oxygen according to

$$O(2^3P)+h\nu\rightarrow O(3^3D) \qquad (1)$$

The produced $O(3^3D)$ atom further passes partly to the continuous level by absorbing the visible radiation (λ 7813Å) and partly to the 3^3P level, emitting the infrared radiation (λ 11287Å) i.e.

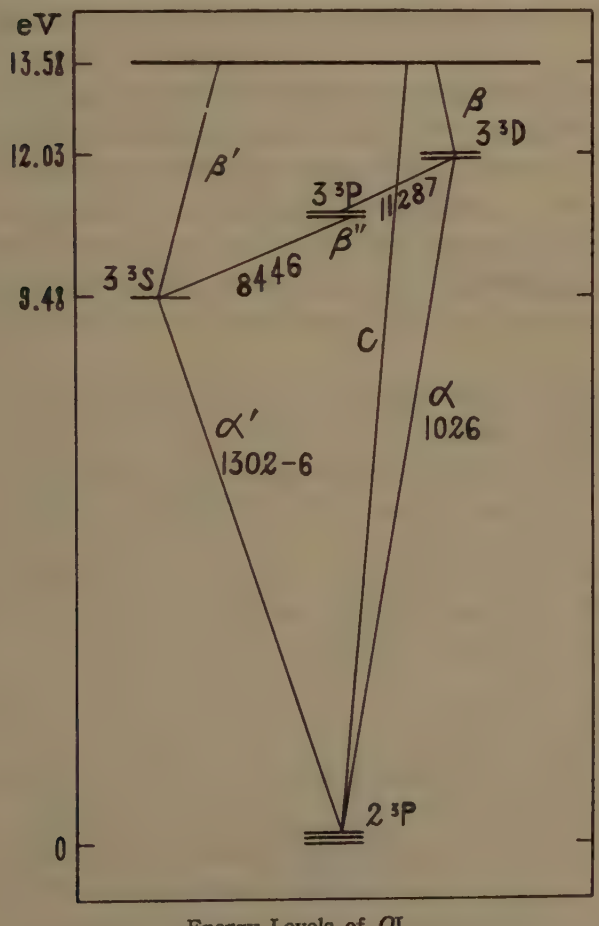

Energy Levels of OI

$$O(3^3D)+h\nu(<\lambda 7813\text{Å})\rightarrow O^+ + e, \qquad (2)$$

$$O(3^3D)\rightarrow 0(3^3P)+h\nu(\lambda\ 11287\text{Å}). \qquad (3)$$

Further we have the following processes

$$O(3^3P)\rightarrow O(3^3S)+h\nu(\lambda\ 886\text{Å}), \qquad (4)$$

$$O(3^3S)\rightarrow O(2^3P)+h\nu(\lambda 1302\text{Å}), \qquad (5)$$

$$O(3^3S)+h\nu(<\lambda\ 3033\text{Å})\rightarrow O^+ + e, \qquad (6)$$

$$O(2^3P)+h\nu(>13.58eV)\rightarrow O^+ + e. \qquad (7)$$

These processes are to determine the feature of the incident solar Lyman beta radiation through the ionosphere.

All of these processes except (2) (6) and (7) make the incident Lyman β-line split into the two scattered radiations i. e. the radiatons 2^3P-3^3D and 2^3P-3^3S, accompanying absorption and emission of the visible as well as the infrared radiations.

Here we must pay an attention to these radiations. For the thermal emission at these wavelengths should be taken into account in the $F2$ layer where tem-

perature has been estimated to be 10^3 K in the order of magnitude. For instance, with temperature of 10^3 K the ratio of the thermal emission from the ionsphere to the incident solar radiation par c.m^2. and sec. is 0.3 at 8446Å and 1.0 at 11287Å; with 2×10^3 K it becomes 5.7×10^2 and 1.5×10^2 respectively, provided that the solar radiation at these wavelengths is that of black body with temperature of 6×10^3 K. Therefore, in such a layer with high temperature the splitting of the incident radiation into two seems to be far less than in the lower layers with lower temperature.

The processes (2) and (6) produce an ion of atomic oxygen through visible radiation. The produced ion will recombine with electron through the radiative recombination or some other recomibinaion reaction suggested by many authors. S. Miyamoto put forward the theory that in the ionosphere recombination radiation would be available for further ionization [3]. This theory has been developed later by Y. Inoue and proved to be relevant [4]. He has considered all possible recombination reactions from theoretical as well as observational standpoints and concluded that the most probable processes are the radiative recombination and the mutual-neutralization, both of which have the same effect on the radiation field apart from their rates and contribute to the scattering of the ionizing as well as the split radiations [4].

We assume that the ionosphere principally consists of atomic oxygen and molecular nitrogen in the E and the F regions. The ionization potential of molecular nitrogen is 15.58 eV, while that of atomic oxygen being 13.58 eV. Furthermore there is no considerable absorption at wavelengths of the two split radiations. Molecular nitrogen, therefore, does not play any important role in our problem. As being the case, the radiation field has no sink in hydrodynamic term throughout the ionosphere down to the region where the appreciable absorption of molecular oxygen takes place.

Now we examine the splitting of the incoming solar $L\beta$ radiation in the lower region following the theory of radiative transfer.

It is assumed that the radiation field is in a quasi-stationary state and varies with the zenith distace of the sun in a slow manner. The equations of radiative transfer are as follows,

$$\cos\theta\frac{dI_\alpha}{d\tau}=w_\alpha\left(I_\alpha-\frac{N_DA_{D1}}{N_1B_{1D}}\right),$$

$$\cos\theta\frac{dI_{\alpha'}}{d\tau}=w_{\alpha'}\left(I_{\alpha'}-\frac{N_SA_{S1}}{N_1B_{1S}}\right),$$

$$\cos\theta\frac{dI_C}{d\tau}=I_C-\frac{N_CN_eA_{C1}}{N_1B_{1C}},$$

where B_{1D}, B_{1S}, B_{1C}, A_{D1}, A_{S1} and A_{C1} are Einstein coefficents of neutral oxygen between the two levels indicated by the suffixes. We denote the four levels i.e. 2^3P 3^3D 3^3S and the contionus levels by 1, D, S, and C, respectively. N_e is electron density, and N_1, N_D, N_S and N_C are number densites in the respective levels. The radiation between 1 and D is named α- radiation, between 1 and S α'-, and between

1 and D C-radiation. τ is optical depth and is defined by

$$d\tau = -N_1 B_{1C} \epsilon dz,$$

where z is a coordinate taken vertically upwards.

$$w_\alpha = \frac{B_{1D}\epsilon_\alpha}{B_{1C}\epsilon},$$

$$w_{\alpha'} = \frac{B_{1S}\epsilon_{\alpha'}}{B_{1C}\epsilon},$$

where ϵ_α, $\epsilon_{\alpha'}$ and ϵ photon energy of α-, α'- and C-radiations respectively. As to θ and I, we follow the usual definition in the theory of radiative transfer in case of the plane parallel layer atomosphere.

The population of each level is determined by the following cyclic equations

$$\frac{\partial N_D}{\partial t} = N_1 B_{1D} J_\alpha + N_C N_e A_{CD} + N_S B_{SD} J_{\beta''} - N_D (A_{D1} + B_{DC} J_\beta + A_{DS}),$$

$$\frac{\partial N_S}{\partial t} = N_1 B_{1S} J_{\alpha'} + N_C N_e A_{CS} + N_D A_{DS} - N_S (A_{S1} + B_{SC} J_{\beta'} + B_{SD} J_{\beta''}),$$

$$\frac{\partial N_1}{\partial t} = N_D A_D + N_S A_{S1} + N_C N_e A_{C1} - N_1 (B_{1D} J_\alpha + B_{1S} J_{\alpha'} + B_{1C} J_C),$$

$$\frac{\partial N_C}{\partial t} = N_1 B_{1C} J_C + N_D B_{DC} J_\beta + N_S B_{SC} J_{\beta'} - N_C N_e (A_{C1} + A_{CD} + A_{CS}),$$

where the subscripts β, β' and β'' pertain to the visible radations between D-C, S-C and S-D respectively. We take four levels, 1, S, D, and C levels into consideration although there is one more level 3^3P located between S and D levels. This procedure would be valid approximately, because thermal radiation from the ionosphere plays a role only in the $F2$ layer and its effect rapidly vanishes in the lower region. And all visible as well as infrared radiations concerning our problem come from outside. We assume their effects to be constant on account of their abundant quantities. Then, the 3^3P level does not appear explicitly, but implicitly through A_{DS} and B_{SD} in the equation. We define as in usual case J_α, $J_{\alpha'}$ J_C, J_β, $J_{\beta'}$ and $J_{\beta''}$ by

$$J_\alpha = \frac{1}{4\pi}\int I_\alpha d\omega, \quad J_{\alpha'} = \frac{1}{4\pi}\int I_{\alpha'} d\omega, \qquad \text{etc.}$$

J_α is composed of the two parts, the incident part $J^*_{\odot\alpha}\exp(-\tau w_\alpha \sec\zeta)$ and the scattered part J, as follows

$$J_\alpha = J^*_{\odot\alpha}\exp(-\tau w_\alpha \sec\zeta) + J,$$

where $J^*_{\odot\alpha}$ is the solar radiation at $\tau = 0$ and ζ is the zenith distance of the sun. The Edington approximation is asumed to be applicable to the scatted part.

Finally we get for the region with $\tau \gg 1$ which corresponds to the E and $F1$ layers

$$\frac{J_\alpha}{J_{\alpha'}} \simeq \frac{w_{\alpha'}}{w_\alpha} \cdot \frac{\dfrac{A_{C1}+A_{CD}}{A_{C1}+A_{CD}+A_{CS}} \cdot \dfrac{B_{SC}J_{\beta'}}{A_{S1}} + \dfrac{B_{SD}J_{\beta''}}{A_{S1}}}{\dfrac{A_{D1}+A_{CS}}{A_{C1}+A_{CD}+A_{CS}} \cdot \dfrac{B_{DC}J_\beta}{A_{D1}} + \dfrac{A_{DS}}{A_{D1}}}$$

Although the coefficients in this formula have not yet been known exactly, the following two cases would be possible.

Case 1 The β'' radiation is more effective than the β and β' radiation.

$$\frac{J_\alpha}{J_{\alpha'}} \simeq \frac{B_{1S}}{A_{S1}} \cdot \frac{A_{D1}}{B_{D1}} \cdot \frac{B_{SD}J_{\beta''}}{A_{DS}} \sim 10^{-8} \ll 1.$$

Case 2 The processes with β and β' radiations play an important role.

$$\frac{J_\alpha}{J_{\alpha'}} \simeq \frac{B_{1S}}{A_{S1}} \cdot \frac{A_{D1}}{B_{1D}} \cdot \frac{B_{SC}J_{\beta'}}{A_{DS}} \sim 10^{-8} \ll 1.$$

From these results we conclude that the incident solar Lyman beta radiaton is almost changed into α'-radiation in this region.

Recently the first successful observation of the Lyman alpha radiation was reported by W.B. Pietenpol and others [5], [6]. Once such an observation is made at higher altitude and in shorter wavelength region our estimation will directly be checked. It is interesting to suggest in this connection that the Lyman beta radiation would hardly be observed except in the $F2$ region with high temperature and further whether or not the α'-radiation with a little longer wavelength than Lyman alpha is observed should be a critical test for our scattering model of the ionosphere.

The author wishes to express his sincere thanks to Profs. M. Hasegawa and S. Miyamoto for their kind direction and encouragement through the work. The author is also indebted to Mr. Y. Inoue for his invaluable suggestions and discussions.

Susumu Kato
Geophysical Institute, Kyoto University,
Kyoto, Japan

References

[1] K. Rawer and E. Argence Phy. Rev. **94,** 253 (1954).
[2] R. v. d. Woolley Proc. of the conference on ionospheric physics, Geophysical research papers No. 11, 273 (1952).
[3] S. Miyamoto Kinkyu-kagaku-hokoku, Kyoto Univ. (1945) (Astrophysical research papers Kyoto Univ.) (in Japanese).
[4] Y. Inoue (will be published in the immediate future).
[5] W. B. Pietenpol, W. A. Rense, F. C.Walz, D. S. Stacey and J. M. Jackson Phy. Rev. **90,** 156 (1953).
[6] W. A. Rense Phy. Rev. **91,** 299 (1953).

On Latitudinal Distributions of Diurnal and Semi-diurnal Components of $h'F2$ of the Ionosphere

A study has been made of the latitudinal distributions of the phase and amplitude of the diurnal and semi-diurnal components of $h'F2$, the minimum virtual height of the $F2$ region.

The data subjected to analysis are the hourly median values of $h'F2$ from 36 world-wide ionospheric observatories in December 1945, and from 39 in June 1946. A harmonic analysis of $h'F2$ in Equinox has already been made by Shimazaki [1], so that we ommitted the analysis of the data in this season.

The results of the a analysis are shown in Figs. 1–8, in which the components are distributed against the geographic and geomagnetic latitudes. General characteristics are summarized as follows:

(i) Diurnal Component

(a) The amplitude is larger in northern hemisphere than that in southern in summer and vice versa in winter. However, the very large value in high latitude is

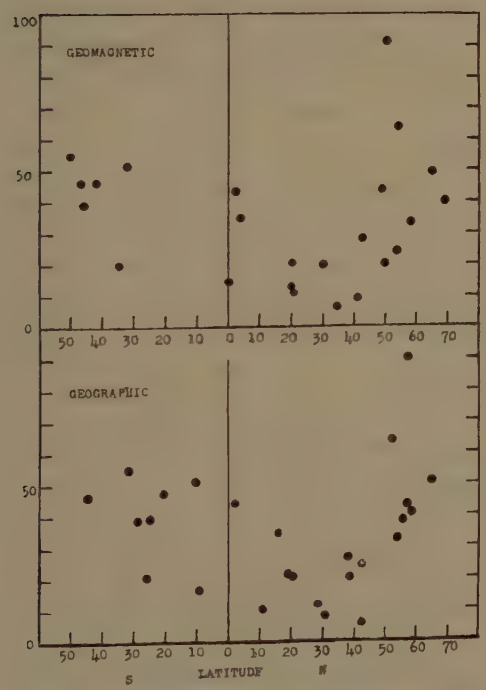

Fig. 1 Distribution of amplitude of $h'F2$ diurnal component in December 1945, plotted against geographic and geomagnetic latitudes.

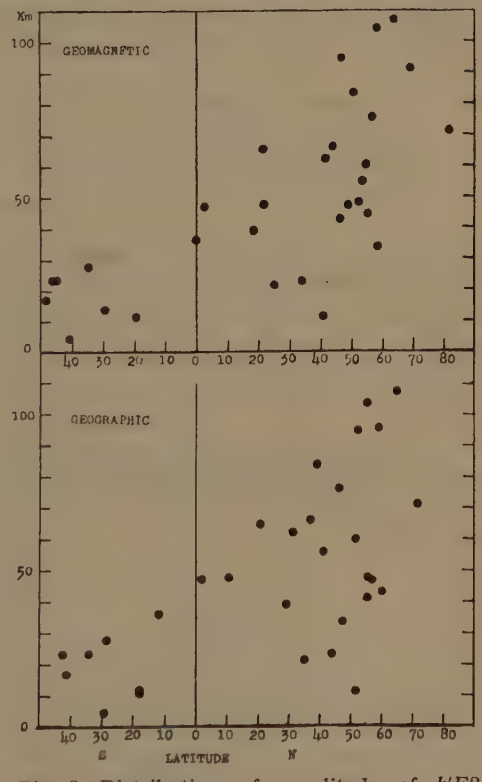

Fig. 2 Distribution of amplitude of $h'F2$ diurnal component in June 1946, plotted against geographic and geomagnetic latitudes.

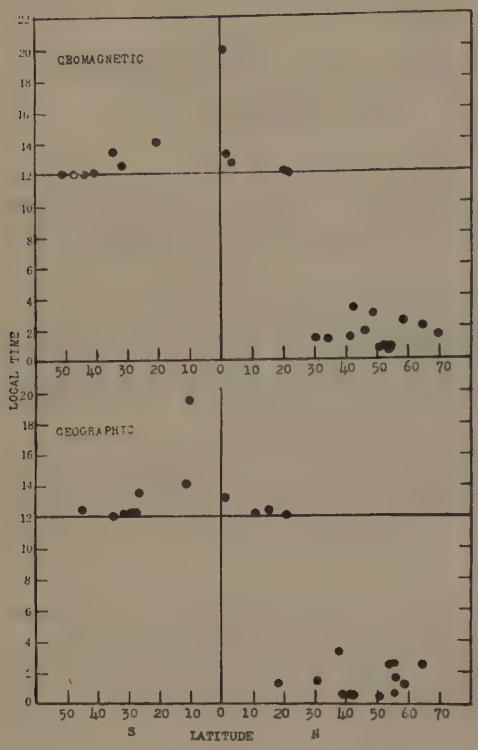

Fig. 3 Distribution of phase of $h'F2$ diurnal component in December 1945, plotted against geogarphic and geomagnetic latitudes.

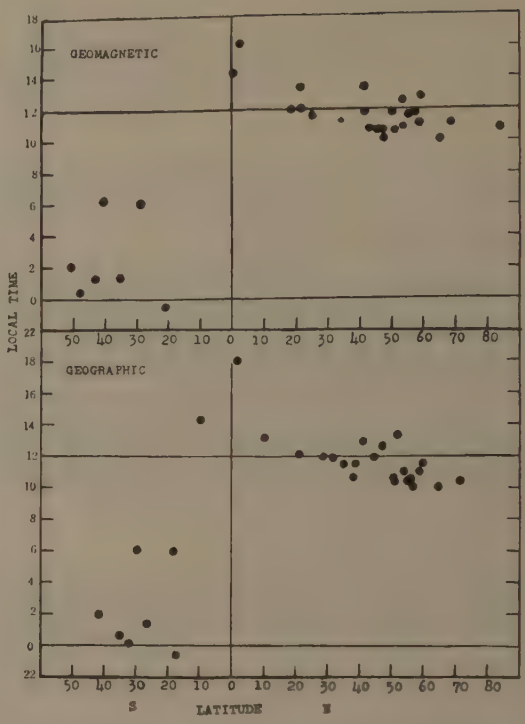

Fig. 4 Distribution of phase of $h'F2$ diurnal component in June 1946, poltted against geographic and geomagnetic latitudes.

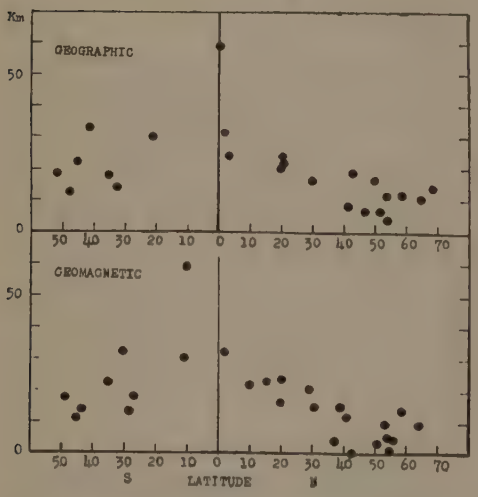

Fig. 5 Distribution of amplitude of $h'F2$ semi-diurnal component in December 1945, plotted against geographic and geomagnetic latitudes.

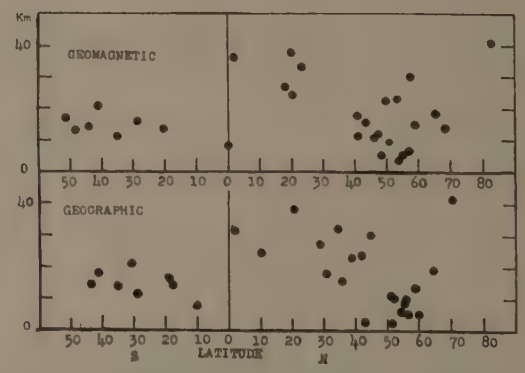

Fig. 6 Distribution of amplitude of $h'F2$ semi-diurnal component in June 1946, plotted against geographic and geomagnetic latitudes.

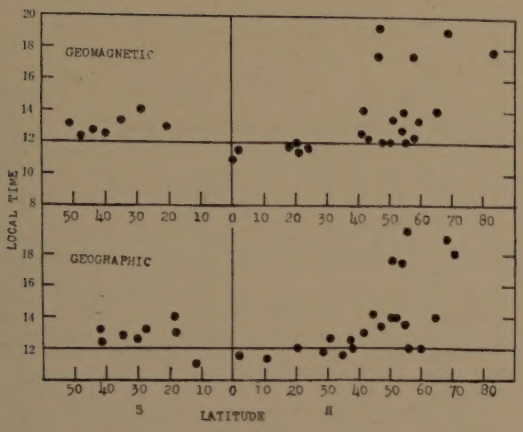

Fig. 7 Distribution of phase of $h'F2$ semi-diurnal component in December 1945, plotted against geographic and geomagnetic latitudes.

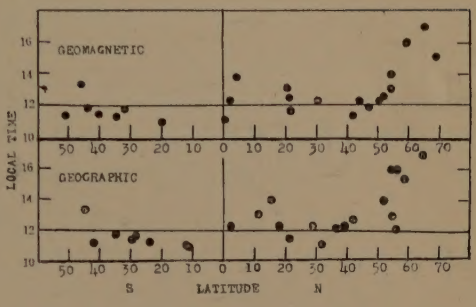

Fig. 8 Distribution of phase of $h'F2$ semi-diurnal component in June 1946, plotted against geographic and geomagnetic latitudes.

considered to be unreliable, judging from the behaviour of the height of the maximum electron density.

(b) The time when the positive maximum occurs is nearly noon in northern hemisphere and midnight in the southern in summer and vice versa in winter. In geomagnetic equator, it seems that there is time lag of 4–6 hours.

(ii) Semi-diurnal Component

(a) The distribution of the amplitude of this component through two hemispheres is analogous to that of the diurnal component, but the magnitude of the former is fairly small compared with that of the latter.

(b) The time when the positive maximum occurs is nearly midnight and noon in summer and winter through two hemispheres. It is considered that, adding the result of analysis by shimazaki, the phase is constant through the year world-widely. There are in some stations at high latitude where the phase lags about 4–6 hours.

By Teruo SATO and Tomikazu NAMIKAWA
Geophysical Institute, Kyoto University

Reference

[1] T. Shimazaki, J. Rad. Resear. Lab., 1, 15 (1954)

昭和30年3月25日　印刷
昭和30年3月31日　發行
第6卷　第3號

編輯兼發行者　日本地球電氣磁氣學會
代表者　長谷川万吉

印刷者　京都市下京區上鳥羽學校前
田中幾治郎

賣捌所　丸善株式會社京都支店
丸善株式會社　東京・大阪・名古屋・仙台・福岡

JOURNAL OF GEOMAGNETISM AND GEOELECTRICITY

Vol. VI No. 3

1954

CONTENTS